EXTRACELLULAR ONCOGENES IN THE DIAGNOSIS AND PATHOGENESIS OF CANCER

By

Saro Aprikian

Department of Experimental Medicine, McGill University, Montreal, QC

July 2019

"A thesis submitted to McGill University in partial fulfillment of the requirements of the degree of Master of Science"

Table of Contents

Abstract

Cancers, with all their hallmarks, are fundamentally driven by genetic events, which can alter the regulatory circuits affecting multiple genes responsible for growth, survival and angiogenesis. It is now known that these specific driver molecules are not confined to the mutant cell but can be emitted to the microenvironment. Depending on their nature, extracellular oncogenes can be released in several forms, such as soluble molecules, molecular complexes, or as cargo of diverse carriers, such as extracellular vesicles (EVs). EVs may contain oncogenes in the context of potentially informative combinations of nucleic acids, proteins and lipids and thus have attracted diagnostic attention as a platform of liquid biopsy. It is often unappreciated that EV release is a regulated process and so is their diagnostic potential. EV release and regulation is also dependant on oncogenic insults, thus implying that oncogenes, to some extent, regulate their own EV-mediated release. We hypothesized that extracellular oncogene emission, and therefore its potential diagnostic applicability, is dependent on the nature of the cancer being studied and the class of oncogenic events driving disease progression. We observed that cancer cells driven by oncogenic RAS release ample amounts of mutant *HRAS* EV-DNA both in vitro and in vivo (in blood). In contrast, oncogenes acting on the cellular epigenome posed higher analytical barriers. For example, the content of mutant *IDH1* in plasma of patients with glioma were found to be highly variable, while tumours driven by oncohistone mutations in *H3F3A* (giant cell tumour of the bone and glioblastoma) released virtually no mutant DNA *in vivo*, while in vitro sequence-specific EV-DNA assays underperformed in comparison to cellular DNA preparations, thus suggesting a structural barrier in detectability. We also show that oncohistone-driven cells of similar tissue origins may differ in the amount of EVs released as well as their histone DNA, RNA and/or protein content. In addition, we observed that prolonged passage in culture and the associated likelihood of cellular reprogramming and transformation may alter the pool of extracellular oncogenes and their EV carriers. While liquid biopsy analytes have traditionally been viewed as being passively and unspecifically released from dying cancer cells, our work documents the existence of regulatory mechanisms whereby viable cancer cells may release oncogenic signals in a manner defined by their transformation and biological state.

Résumé

Les cancers, avec toutes leurs caractéristiques, sont essentiellement provoqués par des événements génétiques qui peuvent modifier des circuits qui affectent plusieurs gènes responsables pour la croissance, la survie et l'angiogenèse. Il est maintenant connu que ces molécules spécifiques ne sont pas confinées à la cellule mutante mais peuvent être émises dans le microenvironnement. Selon leur nature, les oncogènes extracellulaires peuvent être libérés sous plusieurs formes, telles que des molécules solubles, des complexes moléculaires ou en tant que cargaison de vésicules extracellulaires (VE). Ces vésicules peuvent contenir des oncogènes potentiellement informatives en forme d'acides nucléiques, de protéines et de lipides et ont donc attiré l'attention du monde du diagnostic en tant que plateforme de biopsie liquide. Il est souvent méconnu que la libération des VE soit un processus réglementé, de même que leur potentiel de diagnostic. La libération et la régulation des VE dépendent également d'insultes oncogéniques, ce qui implique que les oncogènes régulent, dans une certaine mesure, leur propre libération induite par les VE. Nous avons émis l'hypothèse que l'émission extracellulaire d'oncogènes, et donc leurs applicabilité diagnostique, dépend de la nature du cancer et de la classe des événements oncogéniques conduisant à la progression de la maladie. Nous avons observé que les cellules cancéreuses entraînées par l'oncogène RAS libèrent des quantités importantes d'ADN *HRAS* dans des VE dans les contextes in vitro et in vivo (dans le sang). En revanche, les oncogènes agissant sur l'épigénome cellulaire constituaient des barrières analytiques plus élevées. Par exemple, la teneur en *IDH1* mutant dans le plasma de patients atteints de gliome s'est avérée très variable, tandis que les tumeurs induites par des mutation de l'oncohistone H3.3 (tumeur à cellules géantes de l'os et glioblastome) ne libéraient pratiquement pas d'ADN mutant in vivo, tandis que dans le contexte in vitro, les dosages d'ADN-VE spécifiques à une séquence ont été moins performants que les préparations d'ADN cellulaire suggérant une barrière structurelle en matière de détectabilité. Nous montrons également que les cellules d'origines tissulaires similaires induites par l'oncohistone peuvent différer en quantité de VE libérés ainsi qu'en teneur en ADN, ARN et / ou protéines de l'histone. De plus, nous avons observé qu'un passage prolongé en culture et la probabilité associée de reprogrammation et de transformation cellulaires peuvent altérer le pool d'oncogènes extracellulaires et leurs porteurs VE. Alors que les analytes de biopsie liquide étaient traditionnellement considérés comme libérés de manière passive et non spécifique par des cellules cancéreuses mourantes, notre travail documente l'existence de mécanismes de régulation

permettant aux cellules cancéreuses viables de libérer des signaux oncogéniques d'une manière définie par leur transformation et leur état biologique.

Acknowledgements

I firstly wish to express my deepest gratitude to my supervisor Dr. Janusz Rak and co-supervisor Dr. Nada Jabado for the opportunity they have given me to conduct a master's thesis under their supervision. I wish to particularly thank my immediate supervisor Dr. Rak for his invaluable support, knowledge and mentorship throughout the course of my graduate program.

I wish to also thank my committee members Dr. Andrew Bateman, Dr. Kolja Eppert and Dr. Livia Garzia for their time, support and instructive feedback throughout my master's program.

I also wish to acknowledge my fellow members of the Rak lab: Brian Meehan, Laura Montermini, Shilpa Chennakrishnaiah, Esterina D'Asti, Nadim Tawil, Cristiana Spinelli, Dongsic Choi, Narges Abdian, Lata Adnani, Thupten Tsering and Catherine Pan and sincerely thank them for their constant support and constructive feedback. In addition, I acknowledge several important members of the Jabado lab: Damien Faury, Sima Khazaei and Shriya Deshmukh who have been tremendously kind and helpful throughout my research project.

Finally, I wish to offer my sincere thanks to my family for their constant love and incredible support throughout my academic journey thus far. I therefore dedicate this thesis to my father Armen Aprikian, my mother Paola Aprikian and my brother Alex Aprikian.

Contributions

The data presented in the Results section was generated by me, however, several colleagues contributed to this work in various ways:

Thupten Tsering guided me through the initial extracellular vesicle isolation techniques and also guided me throughout the RAS3-related experiments (Chapter 4). Brian Meehan assisted with mouse injections and blood collections. Nadim Tawil assisted with the western blot experiments. Damien Faury provided cell lines and assisted with the droplet digital PCR assays. Sima Khazaei and Shryia Deshmukh provided cell lines. Nicolas De Jay provided RNA sequencing data (Chapter 6).

List of Figures

List of Tables

List of Abbreviations

2-hydroxyglutarate (2HG)

Arrestin domain-containing protein 1-mediated microvesicle (ARMM)

Blood-brain-barrier (BBB)

Cell-free DNA (cfDNA)

Cell-free RNA (cfRNA)

Central nervous system (CNS)

Cerebrospinal fluid (CSF)

Circulating tumour cells (CTC)

Circulating tumour DNA (ctDNA)

Conditioned media (CM)

Copy number variation (CNV)

Diffuse intrinsic pontine gliomas (DIPG)

Digital droplet polymerase chain reaction (ddPCR)

Dithiothreitol (DTT)

Double-stranded DNA (dsDNA)

Endosomal sorting complexes required for transport (ESCRT)

Extracellular RNA (exRNA)

Extracellular vesicles (EVs)

Food and Drug Administration (FDA)

Genomic DNA (gDNA)

Giant cell tumour of the bone (GCTB/GCT)

Glioblastoma (GBM)

High grade glioma (HGG)

Insertions/Deletion (InDel)

Intraluminal vesicle (ILV)

Limit of blank (LOB)

Limit of detection (LOD)

Log2 fold change (LFC)

Long non-coding RNA (lncRNA)

Micro-RNA (miRNA)

Microvesicle (MV)

Mitogen activated protein kinase (MAPK)

Multivesicular bodies (MVB)

Nanoparticle Tracking Analysis (NTA)

National Institutes of Health (NIH)

Neutrophil extracellular trap formation during inflammatory responses (NETosis)

NOD/SCID/IL2Rgamma-null mice (NSG)

Phosphoinoside-3-kinase (PI3K)

Polymerase chain reaction (PCR)

Polyvinylidene difluoride (PVDF)

Prostate-specific antigen (PSA)

RNA-binding protein (RBP)

RNase H-Dependent PCR (rhPCR)

Ten-eleven translocation (TET)

Tumor susceptibility gene protein 101 (TSG101)

Wildtype (WT)

Xeno Nucleic Acid (XNA)

CHAPTER 1

General Introduction

The Genetics of Cancer

Cancer is a cluster of disease states each involving multiple cellular populations, processes and distinct biological traits. However, there are commonalities permeating this complexity as recently conceptualized by Hanahan and Weinberg (2001) who proposed the distinction of several cancer hallmarks. These hallmarks represent an important conceptual pillar in cancer pathobiology intended to capture the salient phenotypic characteristics of cancer cells and their groupings, such as: the sustaining of proliferative signaling, evasion of tumor suppressors, cell death resistance, metabolic rearrangements, angiogenic potential and other features that occur in multiple cancers regardless of their specific molecular causation (Figure 1.1). Another pillar in understanding cancer has to do with the notion that neoplastic transformation is fundamentally driven by the acquisition of permanent driver anomalies hardwired into the cellular genome or epigenome, mostly in the form of mutations that change the function of genes that control central cellular functions (1). In this sense, cancers can be seen as, in essence, genetic diseases, a notion with significant therapeutic and diagnostic consequences.

Traditionally, cancer-causing mutational alterations have been classified by either the activation (gain-of-function) of oncogenes, or by loss-of-function events, such as the downregulation of tumor suppressors. Both of these classes of changes could be secondary to mutations in genes responsible for the integrity of the cellular genome, the dysfunction of which may lead to increased acquisition of gene variants and ultimately oncogenic mutagenesis (2).

Proto-oncogenes, mostly physiological regulators of cell proliferation and differentiation, can be modified to become oncogenic by several mechanisms such as gene amplifications, intragenic mutations or chromosomal translocations (2). This will result in a selective growth advantage (actual or potential) (3) of the cell harbouring such mutations. The *RAS* oncogene, for example, a frequently mutated oncogene in human cancers, encodes a GTP-binding protein (Ras), a key 'on-off switch' for several important signalling pathways involved in cellular proliferation, survival, migration, expression of angiogenic capacity, immunoregulatory potential and other features (4). In a normal cell, Ras will be transiently activated in order to then initiate pathways such as the mitogen activated protein kinase (MAPK) pathway and the phosphoinoside-3-kinase (PI3K) pathway, which will eventually lead to the transmission of signals responsible for cell growth and survival. Mutations in codons (G12, G13 and Q61) of the *RAS* gene however will render the protein product constitutively active (locked in a GTP-bound state), resulting in abnormal and excessive cell proliferation while ignoring normal mitogenic signals (5).

While aberrations in cellular signalling nodes, such as *RAS*, have been linked to oncogenesis due to their broad impact on the expression of multiple genes and the corresponding changes in cellular functions ('classical' oncogenes), such a pleotropic effect is now known to emerge in several other alternative ways. For example, several classes of cancer-related genes ('non-classical oncogenes') may alter gene expression through their direct effect on the state of chromatin (epigenome), whereby transforming mutations interfere upstream of cellular signalling and within the apparatus responsible for physiological gene repression required for cellular differentiation and proliferative quiescence. For example, mutations in isocitrate dehydrogenase 1 and 2 (*IDH1/2*) will alter the

cellular metabolism in such a way as to affect the methylation state of the DNA (overall hypermethylated DNA), thereby affecting multiple genes and locking the affected cells in a more primitive stem cell-like state. An even more direct effect is that of mutations impacting genes that encode proteins built into chromatin itself, such as histones, where a point mutation may result in the expression of their oncogenic variants ('oncohistones') that no longer obey regulatory mechanisms of cellular differentiation. We will describe some of the relevant features of classical and non-classical oncogenes in more detail in the following chapters.

Tumor suppressor genes act to inhibit cell growth and proliferation in normal cells. Therefore, loss-of-function mutations in these genes will lead to tumorigenesis by eliminating negative regulatory elements in cellular and tissue homeostasis, thereby increasing cell proliferation, formation of the tumour mass and in some cases, metastasis. This usually entails biallelic events or a functional haploinsufficiency of a particular gene. A paradigmatic tumor suppressor mutated in 50% of human cancers is *p53.* This gene product (TP53) is involved in cell-cycle control, apoptosis and maintenance of genetic stability (6). Its protective activity is a crucial reason why mutations in oncogenes such as *RAS* and *MYC* are not sufficient to induce tumorigenesis. Indeed, introduction of mutant Ras into normal cells expressing functional p53 results in cell senescence or apoptosis rather than transformation (7). The loss of this activity can thus be dangerous in relation to cancer, as illustrated by multifocal transformation events occurring in the case of germline *p53* mutations affecting patients with the Li-Fraumeni disease. There are several consequences to this deregulation. First, *p53* loss allows mutant cells to continue through the cell cycle. Second, it enables them to avoid apoptosis. Third, it leads to further genetic instability by allowing additional cancer-promoting mutations to accumulate as cells divide. Notably, the

formation of overt cancer is estimated to entail 3-7 mutational events including oncogenes, tumor suppressors, as well as genes that control genomic stability or senescence (e.g. *TERT*). The cumulative effect of these changes gradually breaks down cellular controls and profoundly changes cellular functions culminating in the expression of cancer hallmarks and the ultimate development of a systemic malignant disease. Moreover, cancer cell lineages progress along multiple clonal evolutionary trajectories resulting in dynamic, spatial and temporal heterogeneity of the resulting lesions (8). In some cancers, these processes of genetic diversification are extremely rapid (9), while in others, the genome remains more quiet, but the abnormalities occur epigenetically, or as a consequence of intercellular interactions (10, 11). In this thesis, we will argue that it is of paramount clinical importance to be able to monitor these changes in real time in individual patients and in a non-invasive manner. The approach or set of technologies known as 'liquid biopsy' represent one of relatively few recognized opportunities (12) to achieve these objectives and we will delve into the exploration of related opportunities as well as barriers.

In summary, the consecutive steps of tumor progression are driven by a succession of mutations that activate oncogenes and inactivate tumor suppressor genes. Different combinations of mutations are required to convert specific cellular populations to their corresponding cancerous counterparts. Moreover, the molecular makeup of cancer cells can be specific to a particular cancer, its subtype or be individual patient-dependant, which mandates individual rather than global diagnoses. Indeed, patients that have the same clinical form of the disease can display different cancer genotypes, a notion that resulted in molecular sub-classification of cancers into distinct subgroups with different biologies and courses of progression. In certain respects, cancers are also unique to the individuals they affect, likely a result of complexity and stochasticity rather

than randomness. Thus, while hallmarks of cancer may be relatively common across the spectrum of malignancies, the underlying molecular apparatus (both targets and biomarkers) could be relatively unique in individual cases. This uniqueness and the temporal dynamics of cancer progression represent a focal point driving the interest in personalized diagnosis and care and a motivation behind this thesis project.

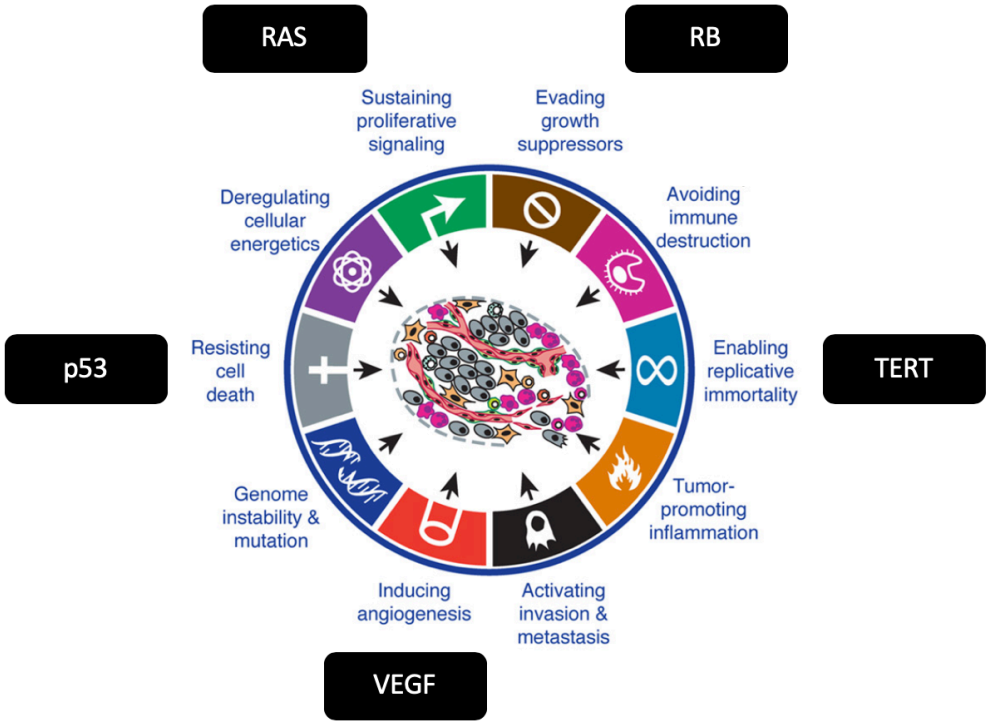

Figure 1.1. The Hallmarks of Cancer and Some Example Genes Mutated. *Adapted from Hanahan and Weinberg. Cell, 2011.*

The Epigenetics of Cancer

While classical oncogenes such as *RAS* have been extensively studied for almost four decades and their modus operandi as well as role in cancer diagnosis reached certain scientific maturity (although far from being resolved), oncogenes acting on the epigenome represent a formidable challenge. A significant part of this thesis project was devoted to this challenge from the diagnostic

perspective. The term "epigenetics" was first coined by Conrad Waddington to describe heritable changes in a cell's phenotype that were independent of alterations in the actual DNA sequence of that cell (13). When speaking of epigenetics, one is usually interested in chromatin. Chromatin is a complex of double stranded DNA wrapped around histone proteins enabling the tight packaging of our entire genome into the small space of the cellular nucleus. A nucleosome is the basic functional unit of chromatin and it contains 147 base pairs of DNA wrapped around an octamer of histones. This octamer is composed of a pair of H2A, H2B, H3 and H4 histone proteins. Chromatin can be either in its active state, termed euchromatin, or in its inactive state, termed heterochromatin. Chromatin is the essential medium through which transcription factors and other cues can alter the genetic activity of a cell (14). Modifications in DNA and histones, such as: methylation or acetylation are dynamically regulated by chromatin-modifying enzymes. These modifications will eventually alter the interactions within and between nucleosomes. Some malignancies harbor mutations in these chromatin-modifying enzymes. For example, follicular lymphomas contain recurrent mutations in *MLL2*, a histone methyltransferase (15).

Sometimes genetic instability can trigger epigenetic instability (Figure 1.2). In other cases, the source of transformation is the epigenome itself. This is the case in gliomas with gain-of-function *IDH1* mutations. Mutant $IDH1^{R132H}$ will produce oncometabolite 2-hydroxyglutarate (2HG) that inhibits the activity of demethylases, including ten-eleven translocation enzymes (TET) (14). Thus, DNA in these gliomas is hypermethylated as a result of an indirect (metabolic) deregulation of methylation enzymes, resulting in tumorigenesis owing to the global change in gene expression (16).

Unlike *IDH1* mutations, oncohistones affect chromatin more directly and from within, which in turn can affect higher-order chromatin states and eventual phenotypic outcomes. Given the fundamental role of chromatin in gene expression regulation, histone-modifying enzymes and chromatin remodeling complexes have been shown to be essential for normal development with their functions affected in diseases such as cancer (17). The role of chromatin in oncogenesis can be illustrated by the discovery of mutations in histone genes (oncohistones), which were never previously considered to be oncogenic. One of the first groups to present this finding was led by Jabado and colleagues (18). They sequenced the exomes of 48 pediatric glioblastoma (GBM) samples and discovered that 31% of tumors had recurrent mutations in *H3F3A*, the gene responsible for encoding the replication-independent histone 3 variant H3.3 (18). These mutations were found to be at two critical positions within the histone tail (K27M, G34R/V) involved in crucial post-translational modifications, notably methylation. They also concluded that *H3F3A* mutations were specific to GBM and highly prevalent in children. It is important to reiterate that this was the first instance where a mutation in a histone-coding gene was linked to tumorigenesis. The following year, in 2013, Behjati et al. reported that mutations $H3F3A^{G34W/L}$ and $H3F3A^{K36M}$ were found in giant cell tumors of the bone (GCTB) and chondroblastomas respectively (19). The proposed mechanisms that drive tumorigenesis as a result of these mutations in H3.3 are linked to the improper deposition of post-translational modifications, specifically methylation. The cumulative effect of these changes in susceptible cellular populations results in a block of cellular differentiation, increase in the stem cell pool and formation of lesions that in some instances (e.g. in the brain) could be highly aggressive, occur early in life and result in the expression of multiple hallmarks of cancer, leading to almost inevitable mortality.

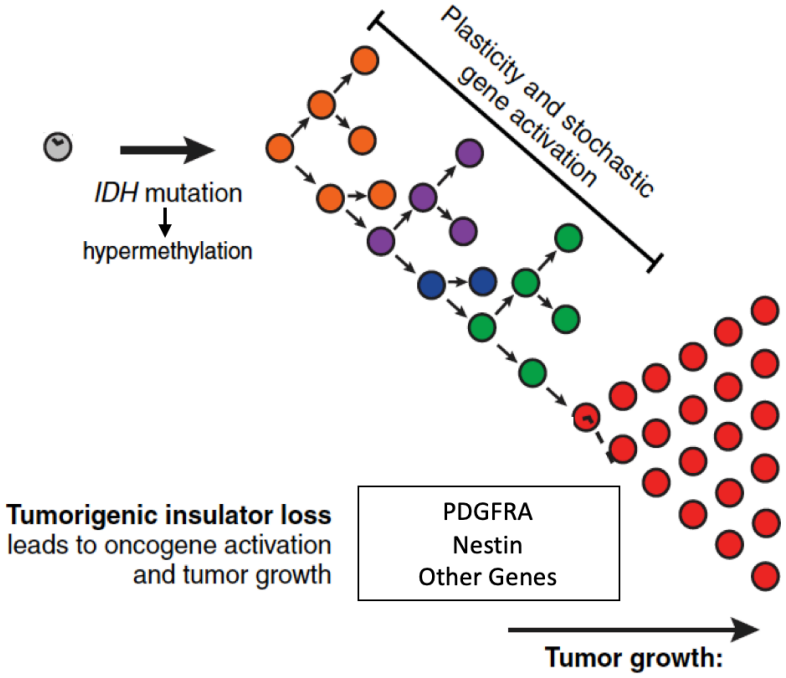

Figure 1.2. Epigenetic Cancer Initiation. An initiating event (e.g., IDH mutation) causes stochastic hypermethylation, leading to a "driver" event that disrupts insulation of oncogenes and as a result, its upregulation. *Adapted from Flavahan et al. Science, 2017.*

Emission of Extracellular Oncogenic Driver Molecules

It has recently come to light that specific oncogenic driver molecules, whether they be in the form of nucleic acids or proteins, are not only confined to the mutant cell, but can also be emitted to the microenvironment. These molecules, depending on their nature, can be released in soluble forms, such as cell-free DNA/RNA or bioactive proteins, as molecular complexes such as RNA-binding proteins and nucleosomes, or as cargo of a diverse repertoire of particles the cells secrete into their surroundings, such as lipoproteins and EVs, as well as debris and apoptotic bodies liberated as a consequence of cellular background (12, 20-22). These processes are of interest as they exteriorize

different molecular forms of oncogenes, notably DNA, RNA and proteins and make them accessible for diagnostic interrogation even without the sampling of cancer cells themselves.

Extracellular DNA has historically been the most studied form of oncogenic material in biofluids. DNA can be released by several mechanisms into the extracellular milieu (Figure 1.3.). These include apoptosis, necrosis and active release, the latter of which is still debated in the literature (23, 24). It is also interesting to note that patients with cancers have more elevated levels of cell-free DNA (cfDNA) than individuals without the disease (25) and more importantly, tumor-related genetic alterations in oncogenes such as *KRAS* and tumor suppressors such as *p53* were consistently detected in the cfDNA of cancer patients (26, 27).

In the case of RNA, the first instance of the detection of this circulating nucleic acid was reported in 1996 by Stevens et al. where they detected tumour-related mRNA in the blood of patients with melanoma (28). Soon after, micro-RNAs (miRNAs) and long non-coding RNAs (lncRNAs) were identified in the circulation of patients harbouring solid tumors (29). It is also important to note that these oncogenic RNAs can be loaded as cargos of EVs where they are protected from the degradation of nucleases. However, in most instances, small RNAs circulate as complexes with RNA-binding proteins (RBPs) (30). Valladi and colleagues (2007) as well as Skog and colleagues (2008) reported an interesting finding where cells, including glioblastoma tumour cells, released EVs containing mRNA and miRNA, both of which can be taken up by recipient cells and further translated (31, 32).

Circulating proteins can also have strong implications in the world of cancer diagnostics. For instance, prostate-specific antigen (PSA) is widely used as a means to diagnose prostate cancer (33). Circulating CA125 levels is used to diagnose and monitor ovarian cancer (34). The two examples above describe instances of soluble proteins in blood. Cell-free proteins may also be associated and transported by EVs. For example, Al-Nedawi and colleagues reported that glioblastoma cells were shown to release the oncogenic mutant form of EGFR (EGFRvIII) in EVs. Not only was this oncogenic receptor loaded into EVs but it was also transferred to other glioma cells while being biologically active, i.e. driving the activation of the MAPK/Akt pathway in recipient cells (35). It is also noteworthy to point out that no clear evidence as to the release of oncohistones to the extracellular environment, and thus their diagnostic potential or paracrine biological activity, has been documented to date. In particular, it is not known whether oncohistones, like classical oncogenes (EGFR, RAS, MET and others), can be released from cancer cells as cargo of EVs (35-37), enter the pericellular space / biofluids and infiltrate recipient cells either in blood or in target organs (38). Neither is it known whether EVs or circulating tumour DNA (ctDNA) present themselves as usable platforms of liquid biopsy analysis or as transmitters of biological activity. These questions and gaps in knowledge motivated the present thesis project largely revolving around the biology of oncogene-carrying EVs.

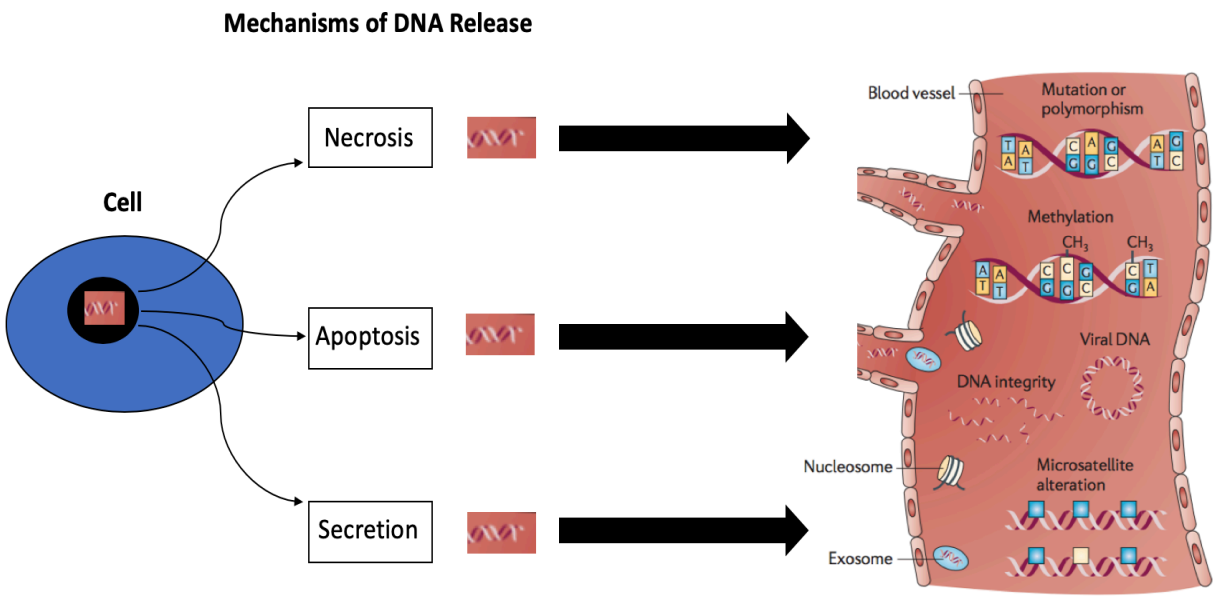

Figure 1.3. Cell-Free DNA: Mechanisms of Release. *Adapted from Schwarzenbach et al. Nature Reviews Cancer, 2011.*

Extracellular Vesicles

Extracellular vesicles are small fragments of cellular content surrounded with plasma membrane and released from cells either spontaneously or as a result of stress, activation or death processes (39). EVs have attracted a great interest in the scientific community as a result of their role in cellular communication and diagnostics. Many researchers have identified these particles in solid tissues (40) and in biological fluids (41). EVs are shed by a myriad of cells including mammalian cells (42), tumour cells (43) and platelets (44) and their numbers in the circulating blood could be as high as 4 x 10^{12} EVs /mL (45).

EVs are heterogeneous in their biogenesis, morphology and molecular makeup, which led to the distinction of their several subtypes, such as exosomes, microvesicles (ectosomes), arrestin

domain-containing protein 1-mediated microvesicles (ARMMs), large oncosomes, migrasomes, in addition to apoptotic bodies and nanosized membrane-less particles such as exomeres (46-48). In many instances, the distinctive features of EVs stem from the biogenetic pathway that gives rise to their formation. For example, microvesicles (MVs) are a class of EVs that bud directly from the plasma membrane and range in size between 100nm - 1μm (49). Consequently, MVs resemble the cells of origin and present surface proteins in a correct orientation while being enriched in integrins, receptors, anexin A1 and phosphatidylserine (50-52). Their formation is not fully understood but some of the molecular regulators include ARF6 and RHOA GTP-ases, acidic sphingomyelinases and lipid scramblases (53). Another EV subtype termed exosomes, typically ranging from 40nm – 120nm in size, are formed by ways of the formation of intraluminal vesicles (ILV) within multivesicular bodies (MVB). ILVs will then be excreted as exosomes upon fusion of the MBVs with the plasma membrane (50, 54). This process is characterized and regulated by the presence of several proteins such as: TSG101, STAM1, ALIX/PDCD6IP and ATG12 (55). The biogenesis of these vesicles is regulated either by the endosomal sorting complexes required for transport (ESCRT) or in an ESCRT-independent manner (56). The latter pathway is regulated by tetraspanins and may be influenced by perturbations in neutral sphingomyelimase activity (NSmase/SMPD3) (57), while intracellular trafficking of exosome precursors (ILVs) is regulated by RAB GTPases and RAB proteins (37, 55, 58). Apoptotic bodies are another class of EVs produced as a result of apoptosis and greatly vary in diameter (50nm - 2μm). A larger subclass of EVs with sizes ranging from 1μm – 10μm that emanate from cancer cells are known as large oncosomes and often carry cancer-specific cargo such as oncoproteins and genomic DNA (59)(60). There is a significant amount of evidence that all classes of EVs may contain oncogenic driver molecules such as: EGFR, EGFRvIII, HER2, RAS and MYC (35, 36, 61-65). The term

'oncosomes' has been coined by our group upon the initial observation of this property (59). However, the same population of cancer cells that secrete EVs harbouring oncogenic proteins may also release oncogene-free EVs, presumably with distinct biological activities (66). Indeed, as mentioned before, EVs can be very heterogeneous in terms of their size, but more interestingly, their cargo as well (Figure 1.3). They may contain lipids, nucleic acids and proteins from the parental cell. Interestingly, both oncogenic (e.g. RAS) (36) and non-oncogenic molecules (e.g. tissue factor) (67) can be included in the EV cargo and transmitted horizontally to recipient cells along with some of the related phenotypic characteristics (35, 36).

EV protein repertoires do not necessarily mimic the cells of origin and can be highly heterogenous. This diversity is due to the fact that, on average, the EV-associated proteome of a cancerous cell population can contain 1000-5000 protein signals. This predicts that if a small EV could be estimated to accommodate up to 200 proteins, the number of non-overlapping EVs subtypes would far exceed the currently known classification (68). Since in reality many proteins can be found in multiple EV subtypes (e.g. CD9), the EV diversity could be very substantial (53). However, certain commonalities do exist (50). For example, exosomes tend to be enriched in tetraspanins CD37, CD53, CD63, CD81 and CD82 (69). Their precursor multivesicular bodies are enriched in ESCRT proteins including tumour susceptibility gene protein 101 (TSG101) and Alix (70). Apoptotic bodies, on the other hand, may have higher levels of DNA-binding histones, integrins, and membrane receptors (71). Indeed, receptor proteins, transcription factors and enzymes associated with EVs drive the functional properties of these EVs and phenotypic changes in the EV-recipient cell. For instance, as mentioned above, in 2008, Al-Nedawi and colleagues reported a finding where glioblastoma cells were shown to release the oncogenic mutant form of EGFR (EGFRvIII)

in EVs, which was successfully transferred to other glioma cells and furthermore activated the MAPK/Akt pathway thus increasing cellular proliferation, survival, colony formation and expression of angiogenic factors (35).

In 2006, Ratajczak first reported the RNA content of EVs (72), and additional seminal studies were soon to follow (31, 32). RNA transported via EVs (EV-RNA) has since been well studied and documented. The amount of RNA in EVs is dependent on the cell type of origin (e.g. cancerous vs. normal cell) (73) and also, EV-RNA profiles do not mimic those of cellular RNA (31), especially in the case of exosomes. Also, as it was eluded previously, several studies have shown the transferability of RNA to recipient cells via EVs with validated translation potential post-uptake (31, 32, 74). However, it remains controversial whether EVs can carry diagnostically and biologically meaningful amounts of noncoding and small RNA, as well as larger transcripts (75, 76). Indeed, while different RNA bioforms have been detected in EVs from various sources (77), the predominant ones include tRNA, piwiRNA, vault RNA and other regulatory subtypes with less mRNA or microRNA (75).

EVs can also carry DNA as cargo (EV-DNA). DNA, specifically, mitochondrial DNA (78), single stranded genomic (73) and double-stranded DNA (dsDNA), ranging anywhere from 100 base pairs (bp) to full-length *HRAS* sequences (3308bp) have been reported in EVs with modal lengths often as high as 6000bp (36, 79). Lee et al. showed that full-length *HRAS* was able to be transferred to non-cancerous recipient cells and remain there for extended periods of time to stimulate increased cellular proliferation. Other oncogenic DNA molecules have also been reported in EVs. *BRAF*,

EGFR, *KRAS* and *p53* DNA were successfully detected in EVs derived from melanoma and pancreatic cancer cells (65, 79).

In summary, given the ample content and biological activity of EV cargo, one must appreciate the contribution of EVs to both cell-cell communication and the growing evidence supporting use of these particles as a biomarker platform in cancer. Notably, the cancer-related and cancer-specific biomarker content of EVs, including all bioforms of classical oncogenes, as well as their detectability in biofluids, suggests for the potential use of EVs in non-invasive diagnostics.

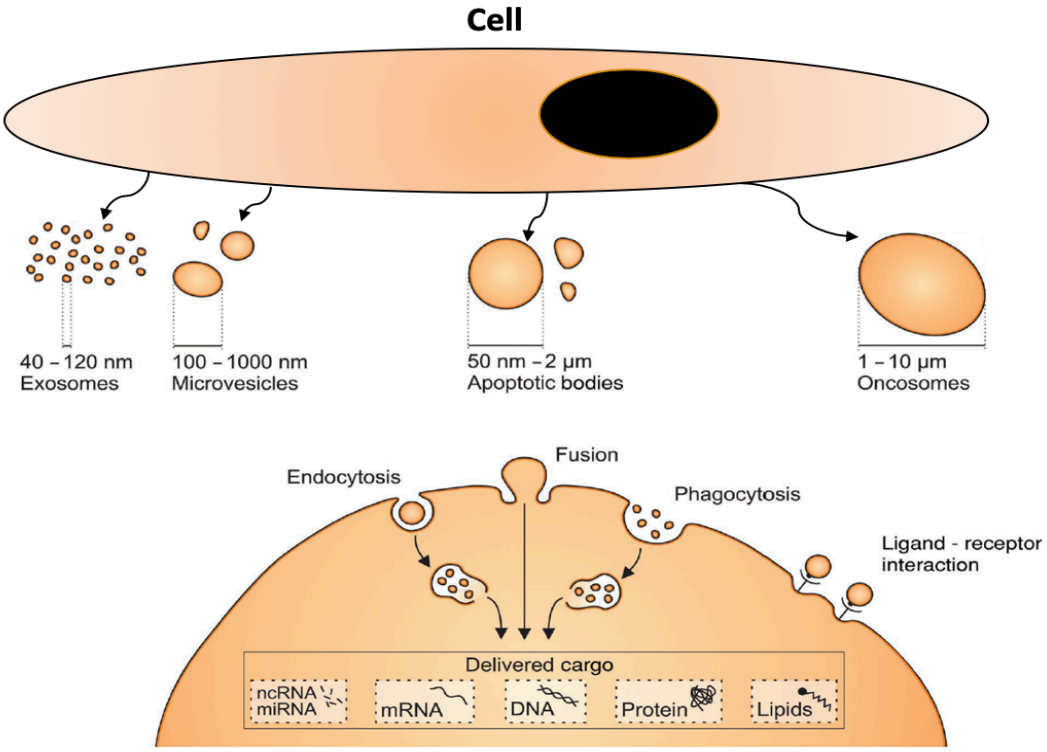

Figure 1.4. Heterogeneity of Extracellular Vesicles. *Adapted from Zaborowski et al. Bioscience, 2015.*

Liquid Biopsy

Tissue biopsies and surgical sampling have and still remain the gold standards for cancer diagnosis. Over the past decade, the pathology component of this approach has been significantly and qualitatively broadened by molecular detail that has, in some cases, revolutionized the nosology and medical decision making, including WHO classification of cancers (80). However, it is important to note that this method has its drawbacks. Firstly, regular biopsy is invasive, painful and sometimes can be contraindicated for medical reasons. Diagnostic biopsy may be impossible for certain cancers with inaccessible lesions, such as diffuse intrinsic pontine gliomas (DIPG) (81), or in disseminated or multifocal disease. Secondly, tissue biopsies may cause unforeseen side effects with sometimes infections occurring, lesion inflammation, bleeding, damage to normal tissue and other detrimental effects. Thirdly, cancers are often heterogeneous, thus leading to subsampling errors in the biopsy process leading to an inaccurate view of the tumour as a whole (8). What's more, a tissue biopsy will only provide a snapshot of the tumour burden at any one time point, typically when a patient is first diagnosed. This poses a problem since tumours evolve genetically with time and through different treatment processes during which they may change their molecular makeup, mutational profile and/or metastasize, thus rendering the initial biopsy findings obsolete. These major issues can, at least in theory, be answered with liquid biopsy, a minimally invasive sampling of a particular biofluid in order to isolate and analyse specific biomarkers shed by tumour cells with the access to the common fluid space (e.g. blood or cerebrospinal fluid – CSF).

There are several biomarker platforms that can serve as portals to access the cancer cell genome, epigenome, transcriptome and proteome. In the context of liquid biopsy, such main platforms of

interest include circulating tumour cells (CTC), cell-free nucleic acids (cfDNA/RNA), tumour-educated platelets, RNA and EVs (Figure 1.5) (12). In addition, our laboratory recently proposed that circulating leukocytes could also serve as carriers of tumour-specific nucleic acids and be adapted as a liquid biopsy platform (38).

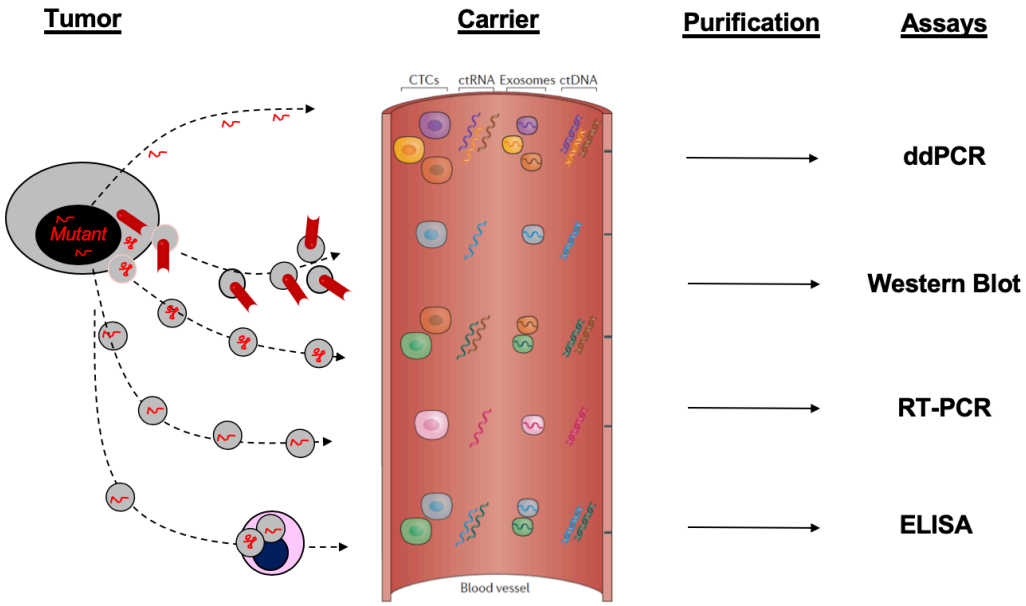

Figure 1.5. Biomarkers Shed From Tumors Into The Bloodstream and Available Analysis Assays. *Adapted from Siravegna et al. Nature Reviews Clinical Oncology, 2017.*

CTCs are tumour cells that have intravasated or have been shed from the primary tumour site or metastatic lesion into the bloodstream (12). The abundance of CTCs in the blood of cancer patients, however, is relatively low (around 1 CTC / $1x10^9$ blood cells) (82), which can be problematic when trying to isolate these cells. It is also worthwhile mentioning that some cancers may not effectively release CTCs into the bloodstream. This is evident in the case of central nervous system (CNS) cancers where the blood-brain-barrier (BBB) poses a significant hurdle in the potential escape of tumour cells into the systemic bloodstream, even though such cells have occasionally

been found (83, 84). If successfully isolated, CTCs can provide very useful information about the molecular profile of the primary tumour, but they unlikely capture the full spectrum of tumour heterogeneity due to low numbers. It is also of note that CTC clusters may represent a more informative biomarker especially in light of the emerging polyclonality of tumour metastases, of which some (not all) CTCs are a point of origin (82).

Cell-free DNA is another very promising biomarker platform in liquid biopsy settings. In 1977, Leon's group reported that cfDNA levels are higher in patients with cancers as compared to patients without the disease (25). Just as it was mentioned previously, cells may release DNA through apoptotic and necrotic processes. In addition to these two 'passive' mechanisms, cells may actively release DNA, as in the case of neutrophils, when undergoing NETosis (neutrophil extracellular trap formation during inflammatory responses) (85-87). Viable cancer cells can also release certain amounts of genomic cfDNA (36) in ways that will be touched on in this thesis project. As a putative biomarker, ctDNA has gathered increasing interest as a means to develop liquid biopsy platforms, and as a result of its several perceived advantages. First, ctDNA has the potential to fully recapitulate the spatial and temporal heterogeneity of the tumor as it is thought to represent the entire cancer cell population with the access to the biofluid space under consideration (e.g. blood). Second, the detection of somatic mutations, insertions/deletions (InDels) and copy number variations (CNV), as well as the evaluation of methylation patterns is demonstrably possible in the case of ctDNA. Third, ctDNA offers a relative ease of isolation, storage, stability and rapid result generation (12). Of course, there are some disadvantages when working with ctDNA, such as degradation and half-life issues, but nonetheless, ctDNA is viewed as one of the most suitable candidate platforms in the domain of liquid biopsy biomarker analysis.

Extracellular RNA (exRNA) is another nucleic acid that received considerable attention in the liquid biopsy space, so much so that National Institutes of Health (NIH) have just completed the first phase of the dedicated multimillion-dollar Common Fund program to study exRNA. Tumour-associated cell-free mRNA was first described in 1996 in the bloods of melanoma patients (28). Subsequently, other forms of RNA, mostly miRNAs and lncRNAs were identified in patients with cancer (29). Tumor-specific RNAs are of major interest and of clinical relevance for reasons such as their ability to identify tumour-related gene-expression profiles (12). Somatic mutations in DNA only represent a subset of possible tumour-associated molecular alterations and cannot fully recapitulate the differences in gene-expression profiles possibly due to epigenetic alterations and miRNA silencing. This is a significant advantage that RNA has over DNA as a potential biomarker.

Finally, EVs can also provide very useful information about the tumour profile and their use as liquid biopsy vehicles is being increasingly appreciated. One aspect of these interests is the ability of EVs to multiplex several independent features of their originating cancer cells such as oncoproteins, lineage markers, responses to microenvironmental stress, therapy and other factors at the DNA, RNA and protein levels (68). A detailed description of EVs was provided previously, but nonetheless, it is important to highlight the heterogeneity of EVs, especially in the context of their cargo. From the biological standpoint, EVs have been shown to contain bioactive lipids, proteins, DNA and RNA, all of which can be horizontally transferred to recipient cells with the potential ability to induce biological changes in the host cells. Therefore, owing to their content, EVs can be exploited as both biological effectors (even drug carriers) and cancer biomarkers (88). An important advantage in regard to EVs is their ability to protect the nucleic acids they contain,

which, when circulating cell-free in the bloodstream, may be subject to degradation by nucleases (60, 89, 90).

Several translational developments have already occurred in the liquid biopsy space. The Food and Drug Administration (FDA) has already approved several biomarkers such as ctDNA for the $EGFR^{L858R}$ mutation (91), Intelliscore exRNA biomarker for prostate cancer (92) and platforms of measuring CTCs for certain indications (81, 93-95). A major study conducted at the Johns Hopkins University by Cohen et al. recently garnered considerable media attention. The authors described a blood test, called CancerSEEK, that can detect eight different cancers through the assessment of mutations in circulating proteins and DNA (96). A total of 1005 patients with clinically detected non-metastatic tumorus went through this test at the time of publication, and the results revealed a few intriguing findings (Figure 1.7). First, cancer detection sensitivities were tumour-specific and ranged from 69% - 98%, where ovarian and liver cancers were most detectable (~98% sensitivity) by the test and breast cancer was the least sensitive (~33% sensitivity). Second, more advanced cancers (stages 2 and 3) were more easily detectable as compared to stage 1 cancers. These findings are in line with the argument (advanced in our work and this thesis) that liquid biopsy techniques and the successes of specific cancer-related biomarkers are dependent on the type of tumour being questioned and the biology of not only the cancer, but also a biomarker-biogenesis process *per se*. This, however, remains an unexplored nexus and one around which our work evolves as described in subsequent chapters.

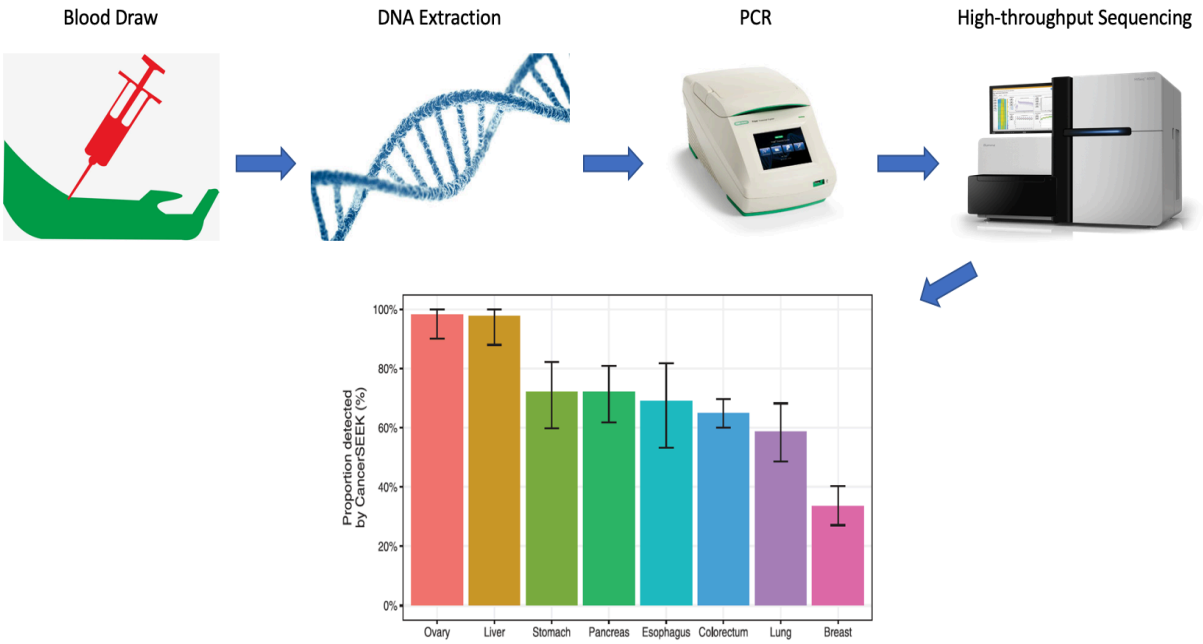

Figure 1.6. Generalized CancerSEEK Protocol and Detection Sensitivity by Tumor Type. *Adapted from Cohen et al. Science, 2018 .*
https://pngtree.com/freepng/blood-test_3331247.html,
https://www.sciencemag.org/news/2018/08/scientists-tweak-dna-viable-human-embryos,
http://www.bio-rad.com/en-ch/product/t100-thermal-cycler?ID=LGTWGIE8Z,
https://www.illumina.com/systems/sequencing-platforms/hiseq-3000-4000.html.

CHAPTER 2

Rationale, Hypothesis and Research Plan

Cancers, with all their cell-autonomous and non-autonomous hallmarks, are fundamentally driven by genetic events, which can alter the functional regulatory circuits that affect multiple genes responsible for growth, survival and angiogenesis (1). While some oncogenic mutations target specific signalling nodes (e.g. RAS), others exhibit a broader impact by targeting the cellular epigenome either directly (e.g. oncohistones) or indirectly (e.g. *IDH1*). It is also known that these specific driver molecules, whether it be protein, DNA or RNA, are not confined to the mutant cell, but can also be emitted into the microenvironment (12). These oncogenic molecules, depending on their nature, can be released in soluble forms, such as cell-free DNA or proteins (cfDNA/protein), as molecular complexes (RNA-binding proteins, nucleosomes) or as cargo of diverse carriers (lipoproteins, extracellular particles) including EVs. The molecular composition of EVs is believed to contribute to the biological activity associated with intercellular transfer of oncogenes and other cargo, and implicated in transient cellular transformation, angiogenesis, thrombosis and other processes linked to EV exchange during cancer progression. While these properties have been mainly studied in the context of 'classical' oncogenes such as HRAS, EGFR or HER2, little is known about processes involving extracellular release of oncogenic chromatin modifiers, such as IDH1 and oncohistones ($H3.3^{G3V/R}$, $H3.3^{K27M}$), the latter crucially involved in pediatric brain tumours, as well as tumors of the bone. Since cancer-related EVs are also present in biofluids at relatively high concentrations, they, along with other carriers of mutant genes, have attracted considerable diagnostic attention as a platform of liquid biopsy. The main emphasis of research in this area has been on overcoming technical sensitivity and specificity challenges, while

the output of oncogene-carrying EVs and particles is often treated as constant (possibly unspecific and passive in nature).

Indeed, in the liquid biopsy space, it is rarely appreciated that EV release is a regulated process and so is their diagnostic potential. EV release and regulation is also dependant on oncogenic insults, thus implying that oncogenes, at least to some extent, regulate their own EV-mediated release. While it has been traditionally assumed that liquid biopsy vehicles, such as cfDNA/nucleosomes, RNA-containing carriers and EVs are constitutively and passively released from the tumour mass, this notion has rarely been rigorously tested, thus raising some important questions: Are different classes of oncogenes equivalent or different in terms of cfDNA/EV-DNA release? Is their entry into the extracellular space/blood passive or is it controlled by the parental cells, the microenvironment, or other factors that may influence liquid biopsy results? Are molecular entities such as mutant DNA equally detectable in cellular and extracellular material? Are there reasons to tailor liquid biopsy concepts to specific tumour contexts in which such assays are to be used?

To begin addressing some of these questions, we **hypothesized** that extracellular oncogene emission, and therefore its potential diagnostic applicability, is dependent on the nature of the cancer being studied, including the nature of the oncogenic mutation, its impact on the affected cell and the tissue/organismal context harbouring these transforming events.

This thesis project studies three different mutant oncogenes: $HRAS^{G12V}$, $IDH1^{R132H}$ and $H3F3A^{G34W/R}$ to assess their extracellular presentation, abundance and detectability of their different molecular forms, especially in the pericellular milieu and blood.

The 3 genes included in this study were chosen carefully. Given its major effect on cellular proliferation and its impact on *in vitro* and *in vivo* aggressiveness, $HRAS^{G12V}$ has been extensively studied in a well characterized cellular model of rat intestinal cancer, RAS3 (description in Materials and Methods) (97). RAS3 cells harbouring the oncogenic $HRAS^{G12V}$ mutation represent an obvious choice as their isogenic non-transformed controls (IEC-18 cells) are readily available as a control. Moreover, RAS3 cells exhibit fulminant tumourigenicity in mice along with all hallmarks of cancer (97) and they release ample ctDNA and EVs both in vitro and in vivo (36, 98). Thus, RAS3 serves as a suitable guide and a stepping stone for the testing and optimization of potential liquid biopsy platforms.

Next, the $IDH1^{R132H}$ mutant adult glioma model was incorporated as a representative of genes relatively frequently mutated in glioma and already having a diagnostic significance in this setting (80). In addition, mutant *IDH1* exemplifies challenges in assessing the interplay between tumour progression, the BBB and the escape of mutant ctDNA into the general circulation. The BBB is a complex protective system composed of specialized endothelium, perivascular and astrocytic layers with a molecular apparatus of intercellular junctions, molecular pumps and other features that isolate and protect neurons in the central nervous system from the circulating blood (99). While there is already evidence for a benefit of CSF-based liquid biopsy over blood in brain tumours (100), the potential of a versatile blood test in this context is worth exploring further and

could be illuminating in relation to the role of the BBB relative to cancer sites where the BBB does not exist.

Finally, the oncohistone models harbouring *H3F3A*$^{G34W/R}$ mutations in GCT and GBM tumours respectively were chosen as there are scarce reports (101) and no established liquid biopsy technology for these mutant cases in the literature to date. This also could provide novel insights into the conceivable use of liquid biopsy measures to monitor tumours driven by epigenetic events.

In practical terms we decided to divide our work into three different blocks (chapters) including:

1- *Analysis of extracellular vesicle-mediated emission of mutant HRAS DNA.*
2- *Analysis of mutant IDH1 levels in plasma samples of human glioma patients.*
3- *Barriers of extracellular release of mutant H3F3A oncohistones from cancer cells.*

Our related findings will be summarized in Chapters 4, 5, and 6 in which we describe stark differences between similar approaches to test extracellular oncogene content in different contexts of cancer cells.

CHAPTER 3

Materials and Methods

Cell Lines and Culture Conditions

This study required the use of several cell lines. The RAS3 cell line represents a related series of isogenic cell lines developed by our lab and that of our collaborators (Dr. Jorge Filmus, Sunnybrook Research Institute, Toronto). RAS3 is a highly tumourigenic variant derived from normal rat intestinal epithelial cells (IEC-18) transformed with the human oncogenic *HRAS* gene carrying a G12V mutation (97) (Figure 3.1). Cell lines obtained from Dr. Jabado include: GCT 5035497 (H3F3A^{G34W}), a primary cell line from a 22-year-old male with giant cell tumor of the bone (GCTB), GCT 1671165-parental (H3F3A^{G34W}) and WT(H3F3A^{G34WT}), the parental being a primary cell line from a 30-year-old male with GCTB with its CRISPR-reverted-to-WT isogenic cell line, and PS10-801 (H3F3A^{G34R}), a primary human GBM cell line from a 15-year-old male. The RAS3 cell line was cultured as a monolayer in AMEM medium with 5% FBS, 1% Penicillin-Streptomycin, 20mM glucose, 4 mM L-glutamine and 10μgml^{-1} insulin. All other cell lines were cultured in DMEM high glucose media (Gibco/Multicell) supplemented with 10% EV-depleted FBS (spin FBS at 34,700 rpm, 4^{O}C, overnight, followed by a 0.22μm filtration step) and 5% Penicillin-Streptomycin. Table 3.1 below summarizes the major cell lines used in this study.

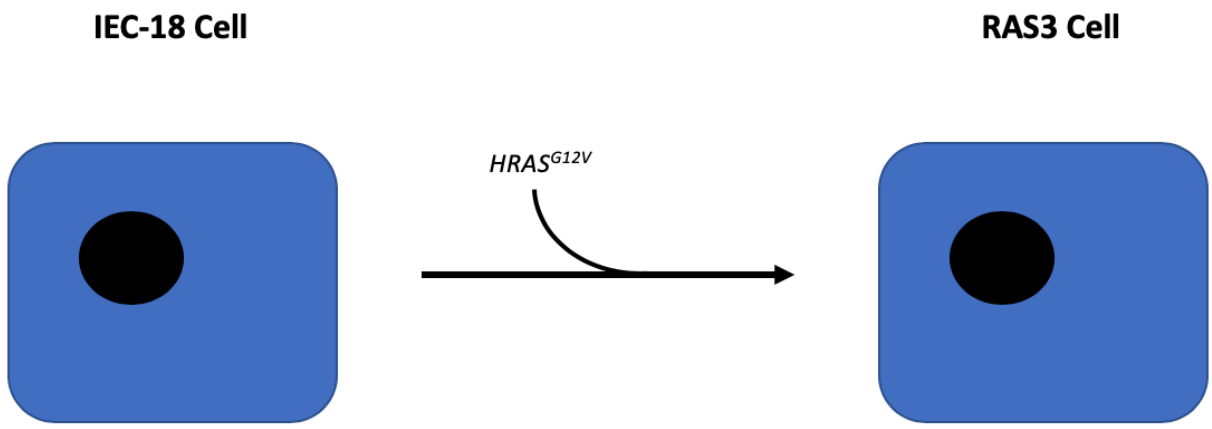

Figure 3.1. Generation of The RAS3 Cell Line.

Cell Line (Full name)	Cell Line (Working name)	Tumor Type	Mutation Status (H3.3)	Patient Age	Patient Sex
GCT 5035497	GCT 503	GCTB	G34W	22	M
GCT 1671165 Parental High Passage	GCT 167-HP	GCTB	G34W	30	M
GCT 1671165 Parental Medium Passage	GCT 167-MP	GCTB	G34W	30	M
GCT 1671165 Parental Low Passage	GCT 167-LP	GCTB	G34W	30	M
GCT 1671165 4C7 WT (CRISPR-ed-to-WT)	GCT 167 ΔG34W **Or** GCT 167-WT	GCTB	WT	30	M
PS10-801	PS10-801	GBM	G34R	15	M

Table 3.1. Summary of Oncohistone-Harboring Cell Lines.

In Vivo Mouse Injections, Tumour Tissue and Blood Collection

All animal procedures were conducted under protocols approved by the institutional Facility Animal Care Committee (FACC) and in accordance with guidelines of the Canadian Council of

Animal Care (CCAC). For RAS3 tumourigenesis assays, YFP/SCID mice were used, developed and bread in house (102). For GCT and glioma cell lines, we used NOD/SCID/IL2R gamma-null mice (NSG) to improve engraftment. A total of 6 NSG mice were subcutaneously injected with 7 x 10^6 Im-GCT-5035497 cells/mouse suspended in Matrigel. Tumours developed within 6 weeks of injection. At clinical endpoint, mice were sacrificed and total blood (~800µl – 1ml) was collected by left ventricle puncture using citrate-coated tubes. Tumour tissues were also collected with part of the tissue samples preserved in formaldehyde while the rest of the samples immediately frozen at -80°C for further analyses. Furthermore, total blood from 3 NSG mice injected in the tibia with 1.5 x 10^6 "10T1/2" cells/mouse (a mouse mesenchymal stem cell line expressing $H3F3A^{G34W}$), were obtained from Dr. Jabado's laboratory.

Mouse Blood Processing

Blood from tumour-injected mice obtained by cardiac puncture was immediately subjected to a centrifugation step at 1,500 rpm for 10 min in order to separate cellular and plasma fractions. Plasma, buffy coat (white blood cells) and red blood cell layers were all collected and stored at -80°C for further analyses as described earlier (38).

Extracellular Vesicle Isolation

EVs were isolated and analysed essentially as recently described (66). Briefly, conditioned media (CM) from all cell lines was isolated at a confluency of approximately 80%. The CM was subjected to a 400xg centrifugation for 5min to pellet remaining cells and debris. A 0.8µm filter was then used to remove apoptotic bodies. Following this was a concentration step using a 100kDa centrifugal filter unit (Amicon Ultra-15, Millipore Sigma) thereby filtering out particles and

molecules >100kDa. The concentrate was then subjected to ultracentrifugation using the TLA 120.2 rotor by Beckman Coulter (110,000xg, 4°C, 1:30 hrs). The EV pellet was then washed with PBS and/or used for further analyses (66).

Nanoparticle Tracking Analysis (NTA)

Nanoparticle Tracking Analysis (NTA, #NS500 NanoSight) utilizes light scattering and Brownian motion to determine the size distribution and concentration of nanosized particles (103). We conducted these assays according to previously published protocols (36, 66, 104). For this purpose, 500µl of CM was isolated from each cell line and subjected to a 0.8µm filtration step before being used for NTA. Samples were loaded onto the NTA chamber and three recordings of 30 seconds were taken under NTA processing settings of the software (NTA version 3.1) to analyze the concentration and size distribution of the particles.

DNA Extraction and Quantification In Vitro From Cell Pellets and EVs

Cell and EV pellets were treated with DNA lysis buffer as described by Laird et al. in 1991 (105) (see below) and isopropanol was used to precipitate the DNA. DNA concentration was determined spectroscopically at 260nm against distilled water as a blank, using the 260/280nm and 260/230nm ratios respectively. Quantification measurements were performed using both the nanodrop spectrophotometer and the fluorometric Qubit system (Thermo Fisher Scientific).

<u>DNA Lysis Buffer</u>

100mM Tris HCl pH 8.5 - 5ml

0.5M EDTA - 0.5ml

10% SDS - 1ml

5M NaCl - 2ml

20mg/ml Proteinase K - 0.25ml

DNA Extraction and Quantification In Vivo From Blood

Plasma obtained from 1 GCTB-diagnosed human patient and the 6 NSG mice injected with Im-GCT-5035497 cells were subjected to DNA extraction using Macherey Nagel's NucleoSpin Plasma XS kit following the manufacturer's instructions. Plasma obtained from 12 patients from Dalhousie University in Halifax (Dr. Conrad Fernandez laboratory) for the *IDH1* liquid biopsy study (as outlined in Results) was subjected to the QIAamp ccfDNA/RNA kit processing (Qiagen) following the manufacturer's instructions. The parallel elution of both cfDNA and cfRNA was possible under these conditions. Buffy coat samples from the GCT-5035497-injected mice were also subjected to a DNA extraction process, this time using the DNeasy Blood and Tissue kit from Qiagen. DNA from tumour tissues were also extracted from all of the above-mentioned experimental animals. In the cases of the GCTB patient and the 6 GCT-5035497-injected NSG mice, the DNeasy Blood and Tissue kit from Qiagen was used following the manufacturer's protocol. In the case of the human tumour tissues obtained from Dalhousie University, we used the Maxwell 16 Tissue DNA Purification kit (Promega). In all cases above, DNA was quantified using both the nanodrop spectrophotometer and the fluorometric Qubit system (Thermo Fisher Scientific).

Polymerase Chain Reaction (PCR)

Regular endpoint PCR was performed using 2µl of genomic DNA preparation containing 10ng of DNA, as a template in order to amplify a 173bp segment of the H3F3A gene containing the

H3.3^{G34W} mutation. The reaction mixture also contained 2x MyTaq HS Red Mix, DNAse free water, 10µM of both forward and reverse primers, and in some cases, differing concentrations of Xeno Nucleic Acid (XNA) clamps (developed by DiaCarta Inc.) amounting to a total reaction volume of 25µl. The primers sequences used are outlined in Table 3.2. The sequence for the XNA clamp used was (5'-GATGACCTCCCCACTTC-3'). The C1000 Thermal Cycler (Bio-Rad) was used to carry out the cycling conditions as follows: 95°C for 5 min and then a cycle consisting of 95°C for 30 sec, if required, an XNA annealing step with a temperature of 70°C for 30 sec, primer annealing temperature of 54°C for 30 sec, 72°C for 1 min. The cycle was repeated 34 times and finalized with a step at 72°C for 5 min. PCR products were then loaded onto a 2% agarose gel, stained with ethidium bromide and ran at 100V in TBE buffer. Separated DNA samples were visualized with the gel documentation system (Bio-Rad).

RNase H-Dependent PCR (rhPCR)

RhPCR is a novel PCR technique that enables an increased precision and more accurate detection of low abundance targets by utilizing unique primers that contain RNA bases in conjunction with a thermostable RNase H2 enzyme. In the case of the *IDH1* liquid biopsy test, we utilized this technology. Briefly, each reaction was comprised of: 2µl of template DNA, 5µl of Evagreen Dye, 0.3µl of each forward and reverse primers at 10µM concentrations, 1µl of RNase H2 enzyme and 1.4µl of DNase-free water. The samples were loaded onto a 96-well plate and passed on to thermal cycling following these conditions: 98°C for 2 min, 10x (98°C for 5 sec, 64°C for 25 sec) and 4°C pause.

Digital Droplet PCR (ddPCR)

Multiple ddPCR assays, both EvaGreen-based and probe-based, were developed for different targets and performed according to the manufacturer's protocols. Briefly, each reaction consisted of differing concentrations of input DNA, QX200 ddPCR EvaGreen Supermix, or probe-based Supermix, 1μM of both forward and reverse primers (sequences outlined in Table 3.2) or a 25x primer-probe mix (in the case of probe-based ddPCR). Probe sequences were outlined in Table 3.3). DNase-free water was used to bring the final reaction volume to 20-25μl. For each reaction, 70μl of Droplet Generation Oil (Bio-Rad) was applied and the oil, along with the samples, were loaded onto cartridges and droplets were generated using the QX100 Droplet Generator (Bio-Rad). The droplets were transferred to a 96-well plate, sealed, and PCR cycling was performed using the C1000 Thermal Cycler (Bio-Rad) with the following conditions. For EvaGreen ddPCR: 1x 95°C for 5 min, 45x (95°C for 30 sec, annealing temperature (all of which are outlined in Table 3.2) for 30 sec, 72°C for 30 sec), and 1x 98 °C for 10 min. For probe-based ddPCR: 1x 95°C for 5 min, 49x (95°C for 30 sec, annealing temperature (all of which are outlined in Table 3.2) for 1 min) and 1x 98°C for 10 min. After PCR reactions were completed, the plate was read using the QX100 Droplet Reader (Bio-Rad) and data were analyzed with the QuantaSoft droplet reader software (Bio-Rad). In the case of the IDH1 liquid biopsy test, each reaction consisted of: 5μl of DNA samples (products of the rhPCR step) diluted 1/5 with low-EDTA TE, 12.5μl of probe-based Supermix, 1μl of 25x primer-probe mix and 6.5μl of DNase-free water. The thermal cycling conditions were: 95°C for 10 min, 45x (94°C for 30 sec, 57°C for 60 sec), 98°C for 10 min and 4°C pause. After PCR reactions were completed, the plate was read using the QX100 Droplet Reader (Bio-Rad) and data were analyzed with the QuantaSoft droplet reader software (Bio-Rad).

Gene and (Primer Notes)	Primer Sequence (5'-3')	Annealing °C
H3F3A (F1/R4 primers)	Fwd: GTACAAAGCAGACTGCCCGCAAAT Rev: GTGGATACATACAAGAGAGACTTTGTCCC	54
H3F3A (Mut-specific primer)	Fwd: GCGCCCTCTACTGGAT Rev: GTGGATACATACAAGAGAGACTTTGTCCC	49
H3F3A (Set #2)	Fwd: GCAAGAGTGCGCCCTCT Rev: GTGGATACATACAAGAGAGACTTTGTCCC	51
H3F3A (Set #3)	Fwd: GCAAGAGTGCGCCCTCT Rev: ACATACAAGAGAGACTTTGTCCCA	54
H-RAS (Human)	Fwd: GCAGGAGACCCTGTAGGAGGACCC Rev: TGGCACCTGGACGGCGGCGCCAG	64
Beta-actin (Human)	Fwd: GGCATCCTCACCCTGAAGTA Rev: CCACTCACCTGGGTCATCTT	58
IDH1 (for rhPCR)	Fwd: AGTGGATGGGTAAAACCTATCATCATAGGT crAT /iSpC3//iSpC3/CA Rev: GTCGTGACTGGGAAAACCCATTATTGCCAACATGACTTACTTGATCCC	64
IDH1 (for ddPCR)	Fwd: GTGGATGGGTAAAACCTATCA Rev: GTCGTGACTGGGAAAACC	57
H3F3A (F1/R5 primers for rtpcr)	Fwd: GTACAAAGCAGACTGCCCGCAAAT Rev: ACCAGGCCTGTAACGATGAGGTTT	56

Table 3.2. Primer Sequences, Amplicon Sizes and Annealing Temperatures Used for PCR/ddPCR and One-Step RT-ddPCR Reactions.

Probe Name	Probe Sequence (5'-3')
H3F3A^{G34W}	WT: HEX/CAC C+C+C +TCC AG/3IABkFQ/ Mut: FAM/CAC +C+C+A +TC+C AG3IABkFQ/
H3F3A^{G34R}	WT: HEX/CAC C+C+C +TCC AG/3IABkFQ/ Mut: FAM/ACC +C+T+T +CCA G+T/3IABkFQ/
IDH1^{R132H}	WT: /5HEX/ATG +A+C+G A+C+C T/3IABkFQ/ Mut: /FAM/CA+T G+A+T +GA+C +CTA/3IABkFQ/

Table 3.3. Probe Sequences for ddPCR and One-Step RT-ddPCR Reactions.

RNA Extraction and Quantification In Vitro From Cell Pellets and EVs

Cell pellets obtained from all cell lines were treated with Qiagen's RNeasy Mini kit by following the manufacturer's protocol for total RNA isolation. EV pellets were subjected to the RNeasy Micro kit, also from Qiagen, following the protocol's instructions for total RNA isolation. All

RNA samples were then quantified using the nanodrop spectrophotometer (Thermo Fisher Scientific).

RNA Extraction and Quantification In Vivo From Blood

Plasma obtained from 6 mice injected with H3.3^{G34W} mutant tumour cells and 1 mouse injected with H3.3^{WT} cells were subjected to RNA extraction using Qiagen's RNeasy Micro Kit following the kit's instructions. Buffy coat samples from the same samples were subjected to RNA extraction, this time using the RNeasy Mini kit from Qiagen. In all cases above, RNA was quantified using the nanodrop spectrophotometer (Thermo Fisher Scientific).

One-Step RT-ddPCR

RNA extracts from cell pellets, EVs, plasma and buffy coat layers were all tested for the H3F3A^{G34W} mutation with the use of Bio-Rad's One-Step RT-ddPCR Advanced Kit for Probes. This assay turns the usual 2-step RT-PCR technique into 1-step, integrating the reverse transcriptase enzyme in the initial reaction mix and having a reverse transcription step part before the regular thermal cycling. Briefly, each reaction consisted of 2 or 5µl of differing concentrations of input RNA, 5µl of Supermix, 2µl of reverse transcriptase, 1µl of 300mM dithiothreitol (DTT), 1µl of target primer/probe mix (sequences outlined in Tables 3.2 and 3.3) and RNase-/DNase-free water to bring the final reaction volume to 22µl. For each reaction, 70µl of Droplet Generation Oil (Bio-Rad) was applied and the oil, along with the samples, were loaded onto cartridges and droplets were generated using the QX100 Droplet Generator (Bio-Rad). The droplets were transferred to a 96-well plate, sealed, and PCR cycling was performed using the C1000 Thermal Cycler (Bio-Rad) using the following conditions: 1x 50°C for 60 min, 1x 95°C for 10 min, 39x

(95°C for 30 sec, annealing temperature of 56°C for 1 min) and 1x 98°C for 10 min. After PCR reactions were completed, the plate was read using the QX100 Droplet Reader (Bio-Rad) and data were analyzed with the QuantaSoft droplet reader software (Bio-Rad).

Western Blot

Cells were pelleted and subjected to the Histone Extraction kit by Abcam as per the manufacturer's instructions for the isolation of total nuclear histones. Lysates were quantified using the nanodrop spectrophotometer using an absorbance of 280nm (Thermo Fisher Scientific). EVs were pelleted by means of ultracentrifugation (110,000xg, 4°C, 1:30hrs) (66) with a subsequent washing step with PBS and further lysed in homemade RIPA buffer (50mM Tris-HCl (pH = 8), 1% NP40, 150mM NaCl, 0.5% sodium deoxycholate, 0.1% SDS, 1mM sodium orthovanadate and 1mM NaF). Lysates were quantified using the Micro BCA Protein Assay Kit (Thermo Fisher Scientific). Proteins were then separated by 12% SDS-PAGE, electro-transferred to polyvinylidene difluoride (PVDF) membranes for 90 min at 4°C (95V) and blocked for 1 hour at room temperature with 5% non-fat dry milk in TBST (pH = 7.5). Membranes were washed and incubated overnight at 4°C with primary antibodies (Table 3.4 lists all antibodies used with respective dilutions). Membranes were then washed three times with TBST for 5 minutes each and then probed with HRP-conjugated anti-rabbit or mouse IgG secondary antibodies for 1 hour at room temperature (Table 3.4). Amersham's ECL prime (Amersham Biosciences) was used for visualization of the X-Ray film that was developed using an automatic film developer.

Primary Antibodies	Dilution	Company and Catalogue #
CD63 (Rabbit monoclonal)	1:1000	Abcam - ab216130
Flotillin-1 (Mouse monoclonal)	1:1000	BD Biosciences - 610821
Total H3 (Mouse monoclonal)	1:1000	Cell Signalling – 96C10
H3.3^{G34W} (Rabbit monoclonal)	1:500	RevMab – RM263
H3.3^{G34R} (Rabbit monoclonal)	1:1000	RevMab – RM240

Secondary Antibodies	Dilution	Company and Catalogue #
Goat anti-mouse IgG (H/L): HRP	1:5000	Bio Rad – STAR207P
Amersham ECL rabbit IgG HRP-linked	1:5000	GE Healthcare Life sciences – NA934-1ML

Table 3.4. List of Antibodies Used.

ELISA

Roche's Cell-Death Detection ELISA^{PLUS} kit was used by following the manufacturer's guidelines. This is specific assay designed to detect cytoplasmic histone-associated-DNA-fragments (mono- and oligonucleosomes) after induced cell death. In the case of the present study, we set out to interrogate the differences in nucleosome concentrations between EVs (pellet) and the soluble fraction (supernatant) of the conditioned media (36). Briefly, EVs from the conditioned media of 1651167 parental-HP cell line were pelleted by means of ultracentrifugation. The supernatant was also collected. At this point 200µl of lysis buffer was added to the EV pellet and a serial dilution was prepared following an incubation step of 30 min at room temperature. Serial dilutions were also prepared for the supernatant. The lysates were then centrifuged at 200 x g for 10 min. Aliquots of 20µl of each of the serially diluted EV lysates and supernatants were transferred along with controls provided in the kit into the microplate coated with streptavidin. To each well containing 20µl of sample, 80µl of immunoreagent was added. The microplate was then

covered with adhesive foil provided by the kit and incubated at room temperature on a plate-shaker at 300rpm for 2 hours. The solution was then removed thoroughly by tapping/blotting on clean tissue sheets. Each well was rinsed with 250µl of incubation buffer (3 times) and 100µl of ABST solution was added. The plate was incubated again on the shaker at 300rpm for 30 min. Finally, 100µl of ABST stop solution was pipetted to each well to inhibit the substrate reaction. The colour reaction in the microplate was then measured at 405nm against ABTS solution + 100µl ABTS stop solution as a blank (reference wavelength - 490 nm).

Data Analysis

All results were repeated at least 2-3 times with error bars integrated in relevant cases, unless otherwise indicated. Student's t-tests were also performed where required to confirm statistically significant differences between datasets. A p-value of 0.05 or less was considered significant.

CHAPTER 4

Analysis of extracellular vesicle-mediated emission of mutant *HRAS* DNA

Introduction and Rationale. Prior work from our laboratory documented a process whereby cfDNA and chromatin are spontaneously released from viable *HRAS*-transformed cancer cells through a pathway involving exosome-like EVs (36, 104). While there is some debate concerning the related mechanism (51), our more recent studies indicated that such a release is a function of the accumulation of the extra-nuclear chromatin in the cytoplasm of *HRAS*-transformed RAS3 cells and this material undergoes EV-mediated extracellular expulsion. In this chapter, we set out to establish sensitive PCR assays to detect these events and to explore how selected experimental variables may impact this readout.

Results and Discussion. In order to shed some light on the nature of DNA release from cancer cells, we employed a rat model of RAS3 cells harboring the human *HRAS* oncogene. In this setting, we interrogated the physical properties (e.g. size) of DNA carriers released from these genetically unstable transformed donor cells. To this end, we conducted a filtration experiment using RAS3 conditioned media and designed to separate larger structures (apoptotic bodies, extracellular micronuclei) from large and small EVs in addition to the soluble fraction, which is ultimately comprised of cfDNA (Tsering, Aprikian, Chennakrishnaiah – manuscript in preparation). DNA was quantified from each of these fractions and Evagreen ddPCR was performed to assay for the presence of *HRAS* copies in each filter fraction. As shown in Figure 4.1, there were stark differences in the *HRAS* signal between different filtered fractions. Thus, in spite of the presence of scarce micronuclei in the RAS3 culture supernatants, the 3μm and 1μm filters retained relatively

little ddPCR signal as did the 0.22μm filter, in spite of certain number of larger EVs (microvesicles) detected earlier in this material. In contrast, the soluble fraction of the RAS3 conditioned medium did contain appreciable amounts of *HRAS* sequences (30-40 copies/ul) suggesting the existence of secretable cfDNA-like material in these preparations. Interestingly, the richest source of *HRAS* DNA was the EV pellet of the culture supernatant, which contained 5-6-fold greater number of copies/μl than the soluble fraction. These observations suggest that EVs contain the highest amount of DNA and *HRAS* copies compared to the negligible amounts found in the remaining fractions, including the flow-through containing soluble cfDNA. It should be noted that RAS3 cells remained highly viable in these experiments (over 95% by trypan blue exclusion) and thus the contribution of cell death to these results is unlikely.

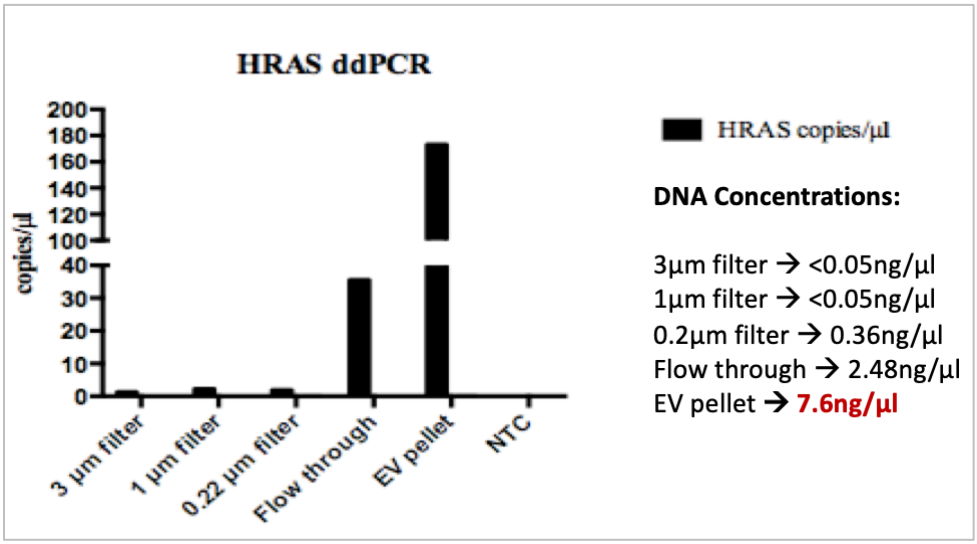

Figure 4.1. Comparison of HRAS Copies/μl in Each Fraction (N=2). The EV fraction exhibits the highest copy numbers of the *HRAS* gene.

Cytoplasmic DNA, which is the likely source of cellular emission of extracellular DNA, was postulated to form through a RAS-driven destruction of nuclear membrane orchestrated by the autophagy machinery (LC3, ATG7) (106). To assess whether this mechanism may contribute to the release of DNA-containing EVs (particles) by RAS3 cells, we treated these cells with

chloroquine, a drug initially known for its anti-malaria effect (107). More recently, chloroquine was shown to inhibit the autophagy process by impairing autophagosome fusion with lysosomes owing to the increased acidity of the latter organelle (108). We therefore assayed the EV preparations from RAS3 conditioned media for *HRAS* copy numbers using Evagreen ddPCR under different treatment conditions. Interestingly, as shown in Figure 4.2, *HRAS* gene quantification using ddPCR suggested that EVs emitted from chloroquine-treated RAS3 cells carried significantly less gDNA in comparison to untreated controls. Moreover, nanoparticle tracking analysis (NTA) showed that chloroquine treatment increased RAS3 EV emission, compared to untreated RAS3 cells. Therefore, the average content of DNA per EV was markedly reduced by chloroquine treatment. Once again, we observed that DNA emission from RAS3 cells occurred at nearly 100% viability. Autophagy-related vesicular transport is multicompartmental. During this process, MVBs may fuse with autophagosomes, thus forming amphisomes, which then may fuse with the lysosome for degradation purposes (109, 110). This may lead to a reduction in EV emission from cells under starvation (111, 112). The entry point for gDNA in the above described pathway is presently uncertain, but in light of our preliminary data, there is a possibility that autophagy contributes to extracellular emission of gDNA (113). It is also worthwhile to mention that in another model (A431), our group documented the association of extracellular DNA with EGFR, collectively suggesting that the emission of oncogenic sequences is not passive or unspecific and may undergo various levels of cellular regulation (35).

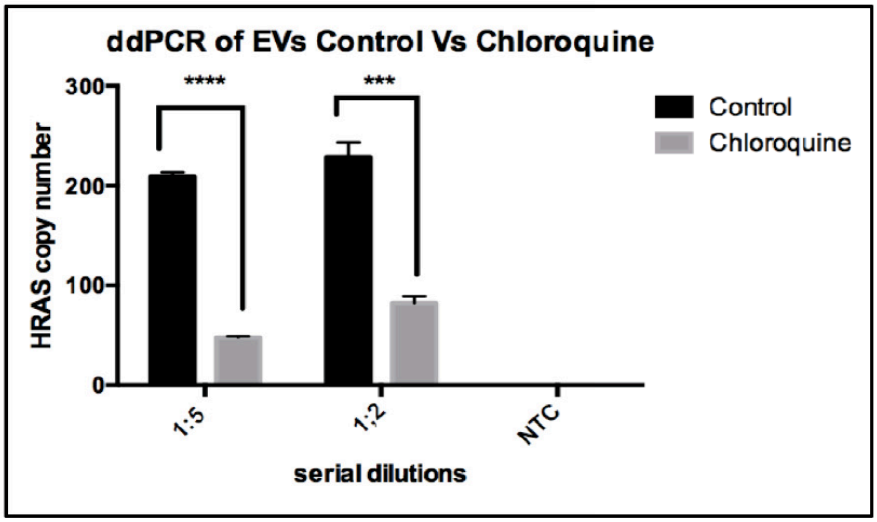

Figure 4.2. ddPCR Analysis of EV-DNA Reveals the Impact of Chloroquine on DNA emission by RAS3 cells (N=3) *(Tsering and Aprikian – 2018).* Serial dilutions (1:2, 1:5) of EVs from untreated and chloroquine-treated RAS3 cells revealing the reduction of *HRAS* copy numbers in the case of EVs released from cells treated with chloroquine.

Because RAS3 cells are highly tumourigenic in mice, they were tested by our group for their ability to release EV-associated and soluble DNA as xenografts in vivo. Indeed, tumour-derived oncogenic DNA was detected in several fractions of blood of RAS3 tumour-bearing mice, including plasma (cfDNA), EVs (EV-DNA) and buffy coats (neutrophil sequestered DNA) (38). Of interest, these studies indicated that biological processes that may impact the levels of circulating phagocytes could influence plasma levels of the *HRAS* signal in cfDNA and EV fractions.

The study on the *HRAS* classical oncogene and its release from cancer cells were designed as a prelude of this thesis project with an intent to validate the experimental protocols and explore the degree and sources of variability in a well-defined experimental system. While RAS3 cells are somewhat artificial, they express several hallmarks of cancer and robustly release all forms of oncogenic signals, including *HRAS* gDNA, RNA and protein into their surroundings (36). They

also release *HRAS*-containing EVs *in vivo*, a process resulting in the loading of this material to circulating leukocytes, as an earlier manuscript demonstrated (38). These processes can be readily monitored and unambiguously interpreted because human *HRAS* sequences can be distinguished from the rat genetic background of RAS3 cells in tumour-bearing mice (98). Our experiments were designed to test two components of this experimental system, namely the predominant fraction in which extracellular DNA-containing oncogenic signal is likely to be found and to explore some of the possible mechanisms of DNA release from these *HRAS*-driven cells. While our results are very preliminary, incomplete and require much further effort, they indicate a regulated model rather than the constitutive release of extracellular DNA and its association with the EV compartment of conditioned media (EV-DNA). We also excluded cell death as a dominant process in generating EV-DNA by careful monitoring cell viability and by documenting that inhibitors of caspases do not reduce EV-DNA release by RAS3 cells (Tsering MSc-thesis, 2018). Most importantly, we established working assays for EV-related and unrelated extracellular DNA detection using a sensitive and quantifiable ddPCR protocol. Thus, the RAS3 model may represent a useful experimental paradigm to investigate the extracellular emission of oncogenes and an opportunity to calibrate ddPCR protocols aimed to detect other oncogenic DNA signatures in the circulating blood.

CHAPTER 5

Analysis of mutant *IDH1* levels in plasma samples of human glioma patients

Introduction and Rationale. Mutation (R132H) of the isocitrate dehydrogenase 1 (*IDH1*) gene is an important classifier (80) and oncogenic driver in a subset of human glioma. These tumours occur usually in younger patients and, paradoxically, exhibit a better prognosis than primary glioblastoma with wildtype *IDH1*. The main mechanism of transformation mediated by this mutation entails a change in cellular metabolism resulting in the production of 2-hydroxyglutarate (2-HG), an oncometabolite that induces widespread changes in the cellular epigenome. Since these are diagnostically important and actionable events, the detection of the cancer-specific $IDH1^{R132H}$ mutational status in liquid biopsy settings would be of great advantage as a means to define tumour subtype, monitor tumour burden and possibly address therapeutic responses in real time. Some efforts in this regard have already been undertaken (114), however, challenges remain. In this chapter, we used efficient PCR protocols to explore whether mutant $IDH1^{R132H}$ DNA is detectable in the blood of patients with glioma.

Results and Discussion. We chose to explore the aforementioned questions through the analysis of the total content of cell-free DNA in plasma of glioma patients, thus including EVs and soluble ctDNA. This project entailed a tripartite collaboration between Dalhousie University (Dr. Fernandez lab) and McGill (Drs. Jabado and Rak labs). Plasma was obtained from a cohort of 16 patients with cancers, mainly glioma, of defined *IDH1* status from Halifax, including different time-points in the disease history. This plasma DNA was then tested, alongside tumour tissue

DNA, for the congruence of the $IDH1^{R132H}$ mutation using an rhPCR pre-amplification protocol, followed by probe-based ddPCR.

We began by establishing the benchmarks of our PCR assay. Limits of blank (LOB) and detection (LOD) were calculated following the protocol reported by Stilla Technologies to ultimately establish the reliable minimum number of positive ddPCR droplets required in order to statistically classify a sample as $IDH1^{R132H}$ mutant. The LOB, the maximum number of plausible false positives with a $1-\alpha$ probability (typically 95% for α=5%), was obtained by first calculating the corrected mean ($\mu_{corr} = \mu + 1.645\ \sigma / R$), where μ is the mean of the non-target samples, σ is the standard deviation from the mean, and R is the number of no target sequence-containing control replicates (in our case, R=36). With the μ_{corr} value calculated, we could now find the LOB by using Table 5.1 (Stilla Technologies). As a result of our $\mu_{corr} = 1.479$, we obtained a LOB of 6.

μ_{corr}	$LOB(95\%)$ in number of positive droplets in chamber
$0 < \mu_{corr} \leq 0.180$	2
$0.180 < \mu_{corr} \leq 0.477$	3
$0.477 < \mu_{corr} \leq 0.863$	4
$0.863 < \mu_{corr} \leq 1.314$	5
$1.314 < \mu_{corr} \leq 1.813$	6
$1.813 < \mu_{corr} \leq 2.348$	7
$2.348 < \mu_{corr} \leq 2.913$	8
$2.913 < \mu_{corr} \leq 3.503$	9
$3.503 < \mu_{corr} \leq 4.115$	10

Table 5.1. Table Using μ_{corr} to Determine LOB. *Adapted from Stilla Technologies.*

Next, in order to calculate the LOD, the minimum concentration that can be non-zero and statistically higher than the LOB with a 1-α probability (typically 95% for α=5%), we used the formula:

$$p_0 = 2b+z^2+z\ \sqrt{(z^2+4b(1-b/N))}\ /\ 2N(1+z^2/N)$$

where:

$b = LOB$ (95%) is the 95% limit of blank

z = 1.645 is the "one-tail" quantile at 95%

N = is the total number of droplets that are generated on average in a chamber (typically N=28000)

p_0 = the higher-value solution of the following equation (which can be simplified as a second-degree equation in p):

$$p = b/\mathrm{N} + \mathrm{z}\sqrt{p(1-p)/N}$$

Finally, once p_0 was determined, we used the formula:

$$LOD_{cp}\,(95\%) = \lceil -N \ln(1-p0) \rceil$$

to obtain the minimum number of positive copies included in the volume analyzed in the chamber. We determined that 12 positive droplets were the minimum amount to consider a sample statistically positive.

Having established the assay, we screened patient plasma samples for the *IDH1*^{R132H} mutation. The results obtained from ddPCR on tumour tissue DNA vs. plasma DNA are summarized in Table 5.2. Out of the 16 patients, tumour IDH1 status was defined for n=12 patients, which out of those 12, n=4 plasma vs. tumour samples were properly matched as *IDH1* WT or mutant.

Sample ID	Tumour IDH1 Status	ddPCR Detection	Diagnosis
A001	R132H (MAF=35%)	++	Diffuse astrocytoma WHO grade II
A003	R132H (IHC+)	-	Anaplastic astrocytoma WHO grade III
A010	R132H (MAF=44%)	-	Recurrent GBM grade IV
A014	R132H (MAF=35%)	+++	Low grade glioma (astrocytoma vs. oligodendroglioma)
A015	R132H (MAF=44%)	-	Low grade glioma (astrocytoma vs. oligodendroglioma)
A002	WT (IHC-)	+	GBM WHO grade IV
A004	WT (IHC-, ddPCR-)	-	GBM WHO grade IV

A005	WT (IHC-)	+/-	GBM WHO grade IV
A006	WT (ddPCR-)	++	GBM WHO grade IV
A007	WT (ddPCR-)	+/-	Recurrent GBM
A011	WT (ddPCR-)	+/-	GBM WHO grade IV
A012	WT (ddPCR-)	-	Melanoma
A009	?	-	Brain metastasis/primary brain neoplasm
A016	?	-	Primary brain neoplasm (oligodendroglial lineage)
A017	?	-	Anaplastic oligodendroglioma WHO grade III
A019	?	-	Anaplastic astrocytoma WHO grade III

Table 5.2. Summary of IDH1 Liquid Biopsy Test Results Obtained Using ddPCR.
+++ = 100 ≤ positive droplets.
++ = 30 ≤ positive droplets.
+ = 14 ≤ positive droplets.
+/- = more or less than ~12 positive droplets at different time points during treatment.
- = < 12 positive droplets.
? = Tumour status unknown.

The above results indicate that *IDH1*^{R132H} ctDNA is released, to a certain extent, into the circulation of human patients. Although only 33% of tumour tissue and plasma samples were matched and ultimately a higher number of matched samples would have been essential for liquid biopsy applications, results can serve as proof of principle that *IDH1*^{R132H} gDNA sequences (like *HRAS*) exit cells and remain in biofluids, such as blood.

However, the poor congruence of tumour versus plasma detection of the *IDH1*^{R132H} mutation reveals an important and presently poorly defined barrier for liquid biopsy approaches. It is presently unclear why congruence was found in some glioma patients and not in others and what factors influenced this variability. Clearly some types of cancers are more easily detectable using means of liquid biopsy compared to others, either as inherent traits of specific cancers, their locations (e.g. behind BBB), clearance of ctDNA or EVs from blood (38, 115), or as a function of analytes and protocols being used. In the case of CNS tumours, CSF is the primary candidate to use as a means for liquid biopsy (116). In contrast, Bettegowda et al. reported that only about 10%

of patients with gliomas harboured mutant ctDNA in the plasma (117). On the other hand, Huang et al. showed that specific H3 gene variant point-mutations can be detected in the form of cfDNA in the CSF with 87.5% sensitivity and 100% specificity (100). Also, another study by Wang et al. concluded that all patients with intracranial high grade gliomas (HGG) adjacent to a cisternal space had detectable levels of ctDNA in the CSF (118).

Therefore, we need to conclude that first, although CSF has proven to be a useful biofluid and platform for liquid biopsy analyses of CNS tumours, there is often clinical hesitation to perform lumbar punctures on patients having intracranial mass given the concern of inducing brain herniation (116), and second, there has not been much success in developing a blood-based liquid biopsy test for CNS-related cancers, which would be the ideal diagnostic test. Because certain numbers of patients with CNS tumours do manifest ctDNA, RNA or EV signals in blood, it is of desirable interest to explore the possibility that, in specific contexts and upon technical refinements, blood-based liquid biopsies could indeed be developed.

CHAPTER 6

Barriers of extracellular release of mutant H3F3A oncohistones from cancer cells

Introduction and Rationale. As described earlier, malignancies involving oncohistones can affect higher-order chromatin states and eventual phenotypic outcomes leading to abnormal development and tumourigenesis (17). The role of chromatin in oncogenesis can be illustrated by the discovery of mutations in these histone coding genes, which was led by Jabado and colleagues (18). However, little evidence and work is found in the literature in regard to developing a working liquid biopsy platform for the detection of such mutations, especially when using blood as the biofluid.

Results and Discussion.

Barriers in Detecting EV-Associated Oncohistone DNA. We set out to adapt a ddPCR assay in order to detect mutant oncohistone DNA sequences. To this end, we were able to access an established primary human cell line (GCT 503) derived from giant cell tumor of the bone, a disease driven by the $H3F3A^{G34W}$ mutation. To assess assay sensitivity, ddPCR was performed on serially diluted cellular DNA samples from this cell line to establish the threshold of specific signal detection (Figure 6.1), which was in the range of 0.2 ng/µl. While this sensitivity should be significantly improved, if the assay was to be used against clinical samples, we wished to first assess whether intracellular and extracellular DNA sources would exhibit comparable performance. This was in part motivated by the notion that chromatin included in the cytoplasmic and extracellular compartments, such as EVs, may be subjected to conditions that could lead to fragmentation and formation of complexes that could impact the performance of the assay. Indeed,

Figure 6.2 shows the results obtained using the same ddPCR assay applied to EV-DNA. It is evident that there is a significant drop in mutant EV-DNA copies/µl as compared to cellular DNA at the same nominal concentrations. It should also be noted that significant amounts of EVs were isolated, as reported in the Nanoparticle Tracking Analysis (NTA; Nanosight NS500) report graph in Figure 6.3. Thus, poor detectability of EV-DNA (*H3F3A*^{G34W} sequences) was not a function of impaired vesiculation. It should also be noted that EV-DNA is known to cover the entire genome (36) and therefore, it is unlikely that *H3F3A*^{G34W} sequences were selectively excluded from this material.

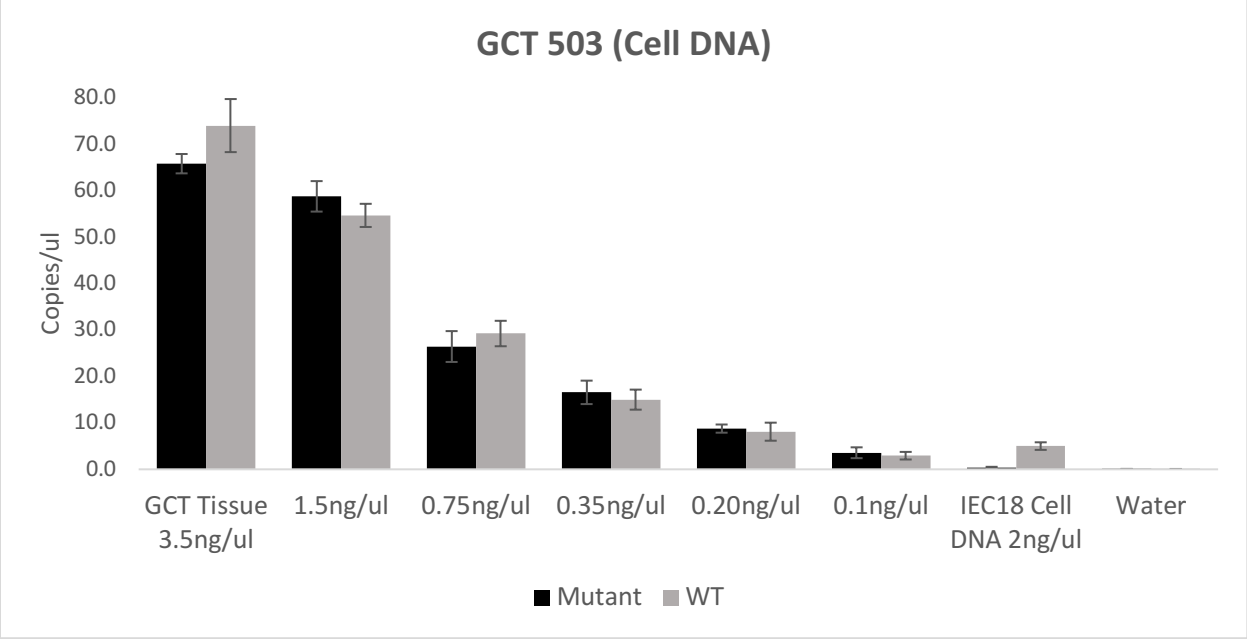

Figure 6.1. Probe-Based ddPCR on GCT 503 gDNA Using Serial Dilutions (N=3). *GCT Tissue = Patient tumour tissue establishing GCT 503 cell line*. **Mutant** = H3F3A^{G34W} mutant. **WT** = H3F3A^{G34} wildtype.

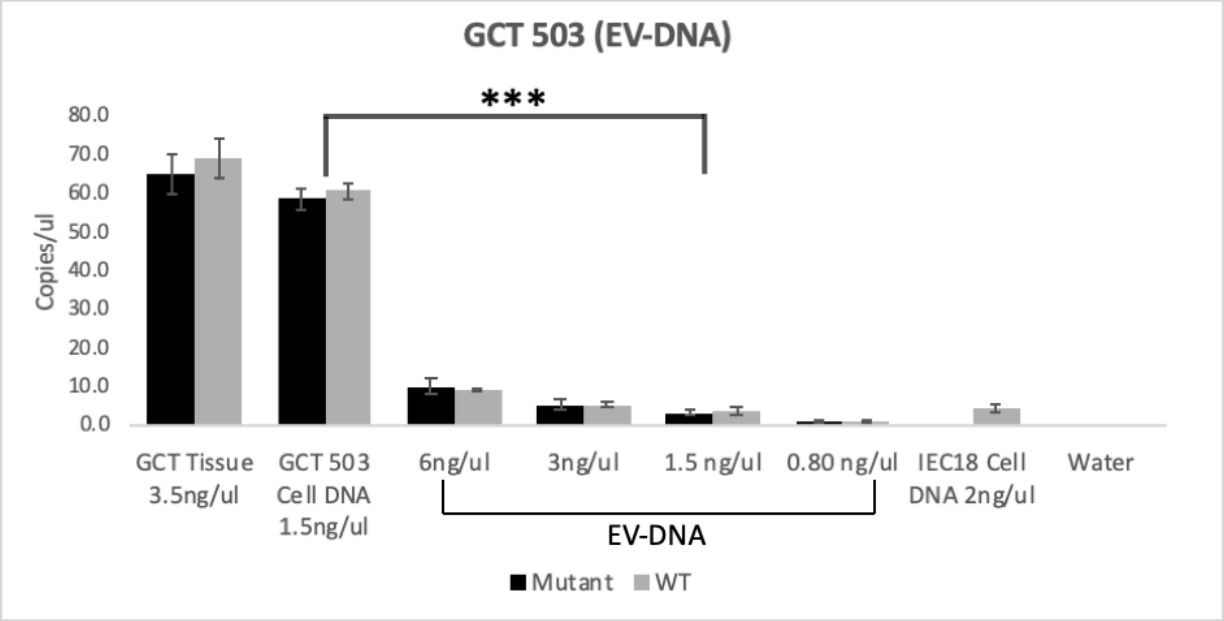

Figure 6.2. Probe-Based ddPCR on GCT 503 EV-DNA Using Serial Dilutions (N=3). Mutant = H3F3A^{G34W} mutant. *GCT Tissue = Patient tumour tissue establishing GCT 503 cell line.* **WT** = H3F3A^{G34} wildtype. *** = *p-value < 0.0005.* This assay shows the significant drop in *H3F3A*^{G34W} EV-DNA as compared to gDNA at the same nominal concentration.

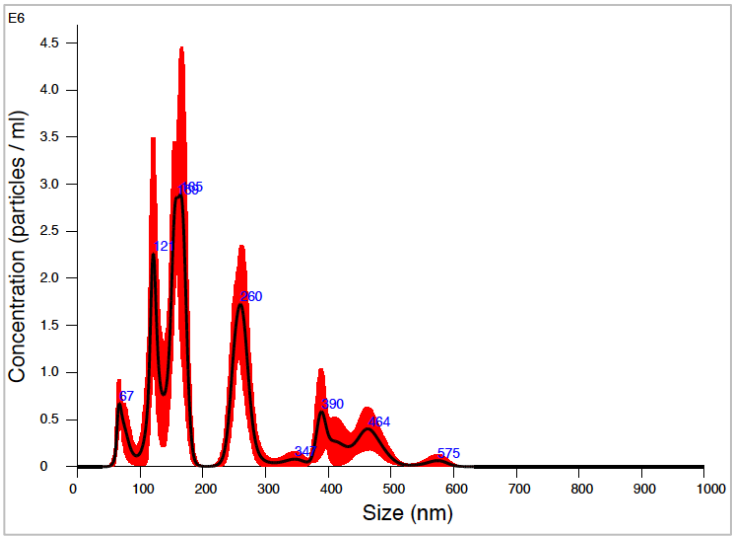

Figure 6.3. GCT 503 EV Size Distribution by NTA.

In order to understand why the same amount of intracellular and extracellular DNA yields different *H3F3A*^{G34W} signals using the same ddPCR assay, we considered several possibilities. We first

reasoned that this could be related to the design of the ddPCR reaction. This therefore prompted us to redesign the assay by including a mutant-specific primer for the *H3F3A*^{G34W} sequence that would enable for the specific amplification of mutant DNA. However, this did not improve the LOD (Figure 6.4).

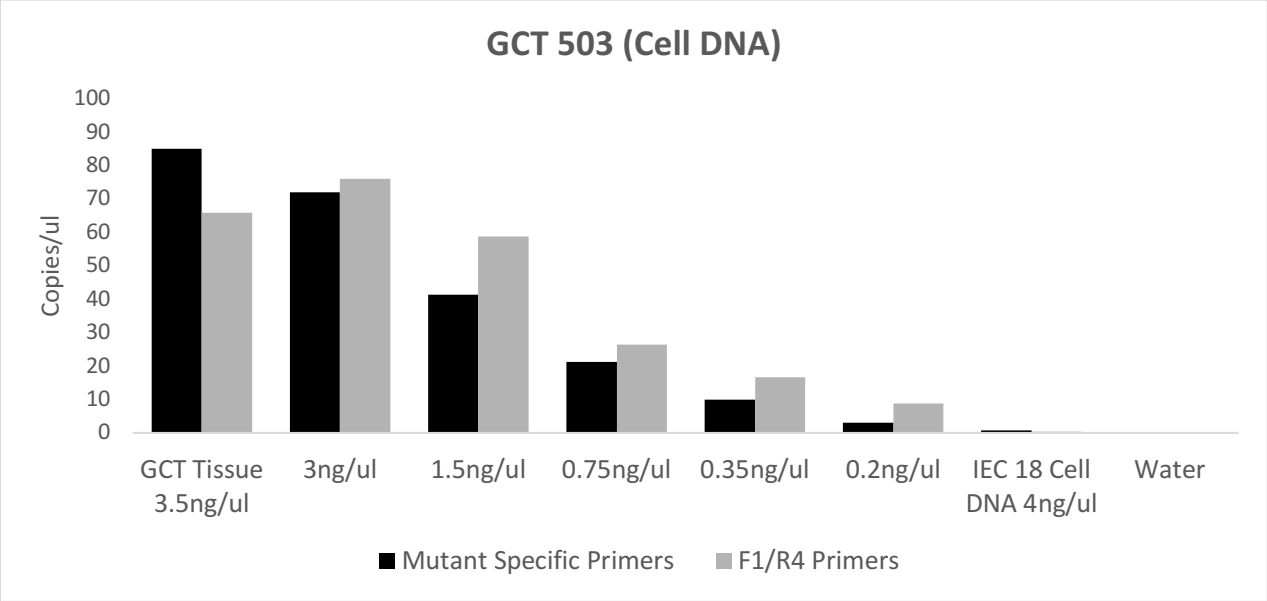

Figure 6.4. Mutant-Specific vs. Regular Primer Evagreen ddPCR on GCT 503 gDNA With Serial Dilutions (N=1). *GCT Tissue = Patient tumour tissue establishing GCT 503 cell line*. This experiment reveals that the mutant-specific primer does not significantly increase the amplification of the mutant allele as compared to the F1/R4 primers used in previous ddPCR assays.

While seeking additional improvements, we then reasoned that this detection inefficiency might be due to EV-DNA fragmentation as a consequence of DNA packaging into EVs. Indeed, our laboratory previously determined the profile of DNA fragments recovered from EV preparations of cancer cells (36). As a result, we tested two other primer sets with smaller amplicon lengths to try to target smaller amplicon fragments in order to establish a better LOD. The results, as shown in Figure 6.5, did not lead to a significant improvement. We then sought out to perform an EV-DNA fragmentation profiling assay using Agilent's Bioanalyzer to confirm if fragmentation was an issue. Figure 6.6 indicated that, while fragmentation did occur, as expected, we were not dealing

with fragments smaller than ~8000bp, ruling out the notion that a smaller-amplicon-length-ddPCR assay would markedly improve detection.

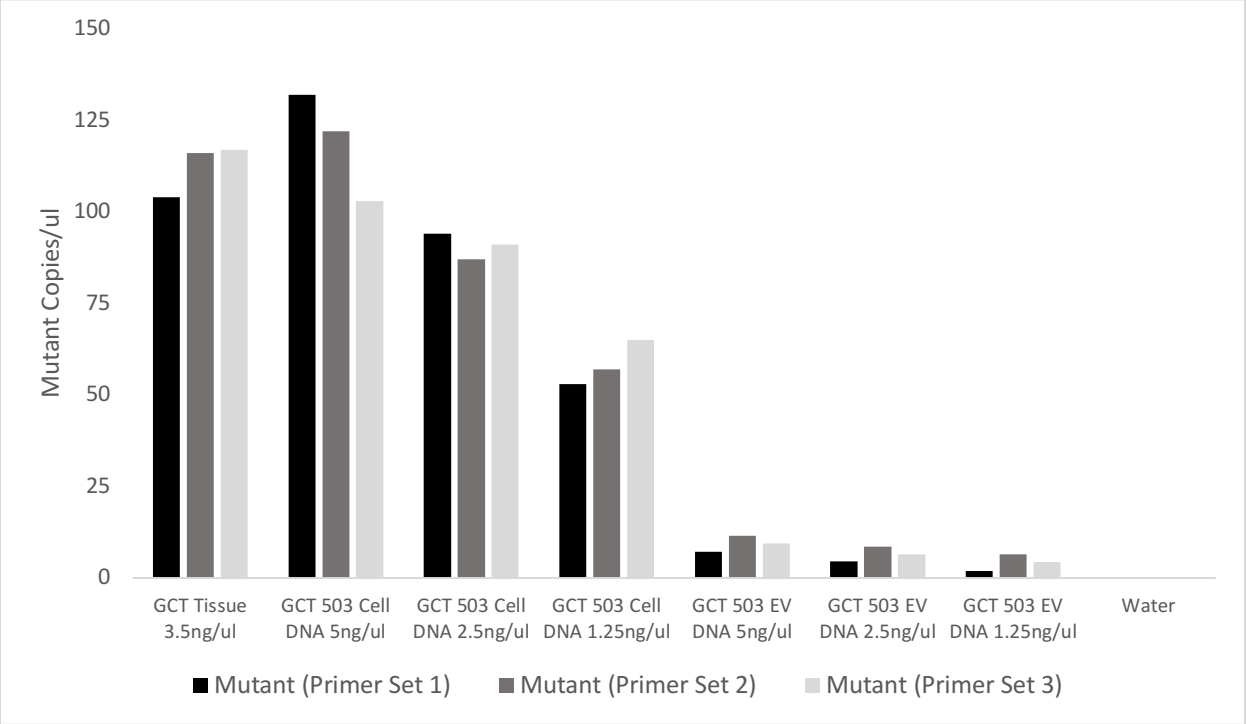

Figure 6.5. Amplicon Length Evagreen ddPCR Test on GCT 503 gDNA vs. EV-DNA With Serial Dilutions (N=1). *GCT Tissue = Patient tumour tissue establishing GCT 503 cell line.* In this ddPCR experiment we observe no significant difference in mutant allele amplification when testing different primers with differing amplicon lengths in both gDNA and EV-DNA cases.

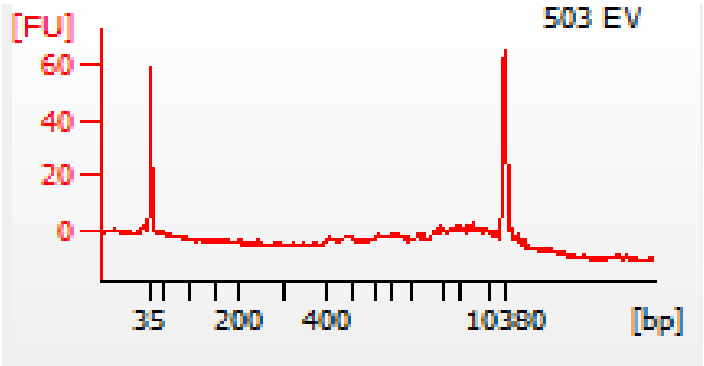

Figure 6.6. GCT 503 EV-DNA Fragmentation Profile Using Agilent's Bioanalyzer.

Our third and final optimization strategy was to apply a highly sensitive PCR clamping assay using

Xeno-nucleic acid (XNA) technology. To this end, we initiated a collaboration with DiaCarta Inc. to design a *H3F3A*^{G34}-specifc XNA clamp in hopes to decrease WT allele expression, while simultaneously increasing mutant allele amplification. We tested this newly-designed XNA clamp on a CRISPR-reverted-to-wildtype cell line (GCT 167 ΔG34W), which has been engineered to express both *H3F3A* alleles as WT. Unfortunately, while this assay is commercially used for other gene sequences, in the case of *H3F3A*^{G34}, the XNA clamp did not meet the expected benchmarks in that we observed multiple amplification bands without a suppression of the WT sequences. This assay is based on a clever strategy and has worked in a number of settings (119), but it clearly needs more refining and optimizing since the PCR in Figure 6.7 shows that the WT alleles were not effectively suppressed. As many aspects of this technology are proprietary, we were unable to pursue this further.

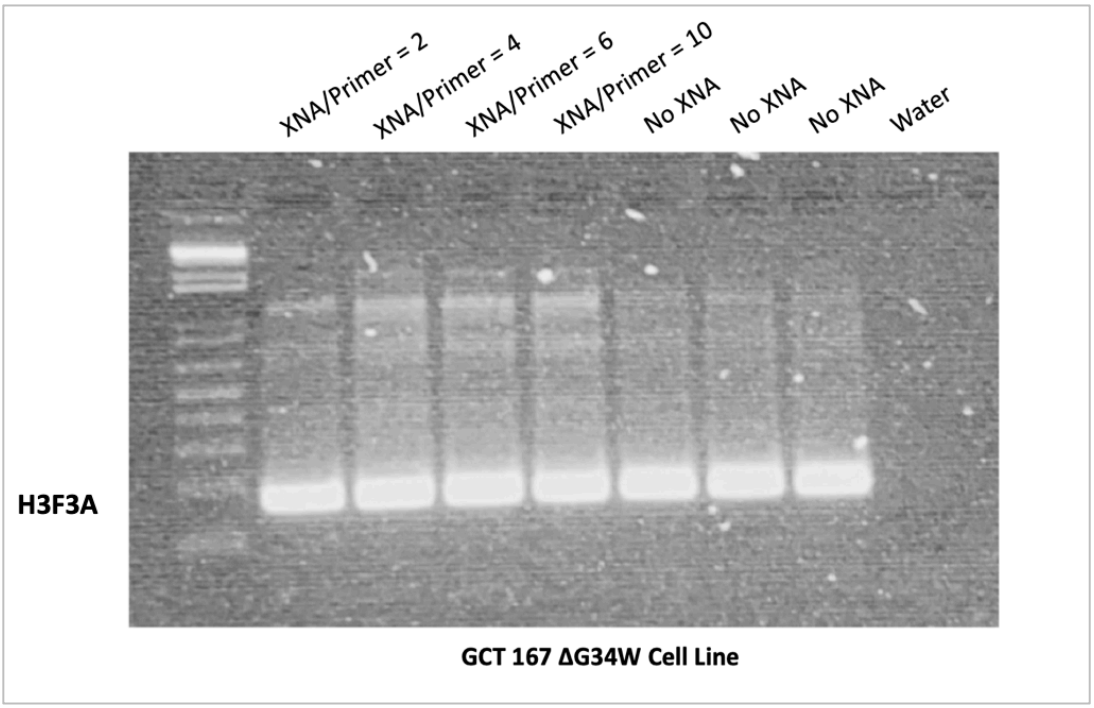

Figure 6.7. XNA Clamp Test Using PCR. This PCR reveals that the XNA clamp is not properly hindering the amplification of the wildtype allele. This is reasoned as a result of the non-noticeable difference in *H3F3A* band intensity in both XNA and no XNA clamp cases. In addition, increasing the XNA/primer ratio did not change band intensity either.

It seems possible that EV-associated DNA possesses features that are qualitatively different than preparations of cellular genomic DNA and incompatible with the current ddPCR protocols, which considerably underperform in the case of this material. However, it cannot be excluded that cfDNA in blood, which is widely used in liquid biopsy studies, possess properties more amenable for ddPCR detection than EV-associated genomic sequences (e.g. lesser or differentiated fragmentation). These questions remain to be resolved more fully.

Intercellular Variation in EV-Mediated Release of Oncohistone DNA. It clearly seems, from previously mentioned results, that cellular contexts impact EV-DNA release and therefore may influence liquid biopsy performance. For example, in the case of the RAS3 cell line, we observed a robust release of DNA-containing EVs, but this was clearly not the case for GCT 503 cells, and may not apply to other cancer contexts. To explore the potential differentials in detecting EV-DNA between cancer cells, we set out to test oncohistone mutations from 3 additional cell lines (descriptions outlined in Materials and Methods, Table 3.1). Although these cells are closely related, 3/4 are derived from GCTs and 2 out of those 3 are clonally related, however, the amount of EV-DNA they released was markedly different. Thus, while in all cases the EV-DNA signal was weaker than the cellular DNA signal, this was particularly pronounced in the case of GCT 503 and less so in GCT 167-MP, while in GCT 167-HP and GCT 167-WT, the detection of *H3F3A* in cells and EVs was more comparable. The results clearly indicate that, as hypothesized, there is a cell-line specific differential in EV-DNA detection (Figure 6.8). In addition, it was also observed that passage number may affect extracellular DNA detection levels with the high passage GCT 1671165 cells (GCT 167-HP) having significantly more $H3F3A^{G34W}$ EV-DNA in their secretome as compared to its lower passage counterparts (GCT 167-MP / LP). Also, in this case, we

performed DNA fragmentation profiling from EVs of all the cell lines used (Figure 6.9) and the profiles were comparable.

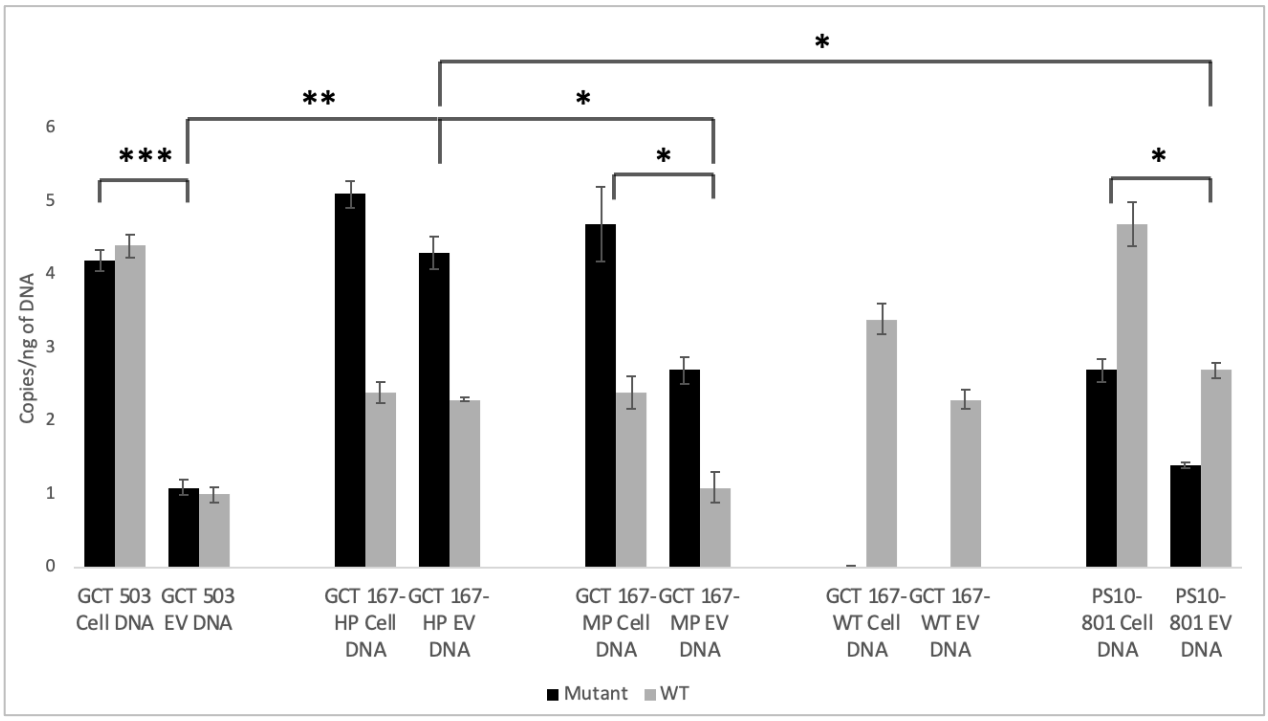

Figure 6.8. Cell Type / Passage-Dependent Differential in EV-DNA Detection (N=3). Mutant = H3F3A^{G34} mutant. **WT** = H3F3A^{G34} wildtype. **HP** = High Passage (> 25), **MP** = Medium Passage (15 < Passage Number < 25), **LP** = Low Passage (< 15). * = *p-value < 0.05,* ** =*0.05 > p-value > 0.005,* *** = *p-value < 0.0005.*

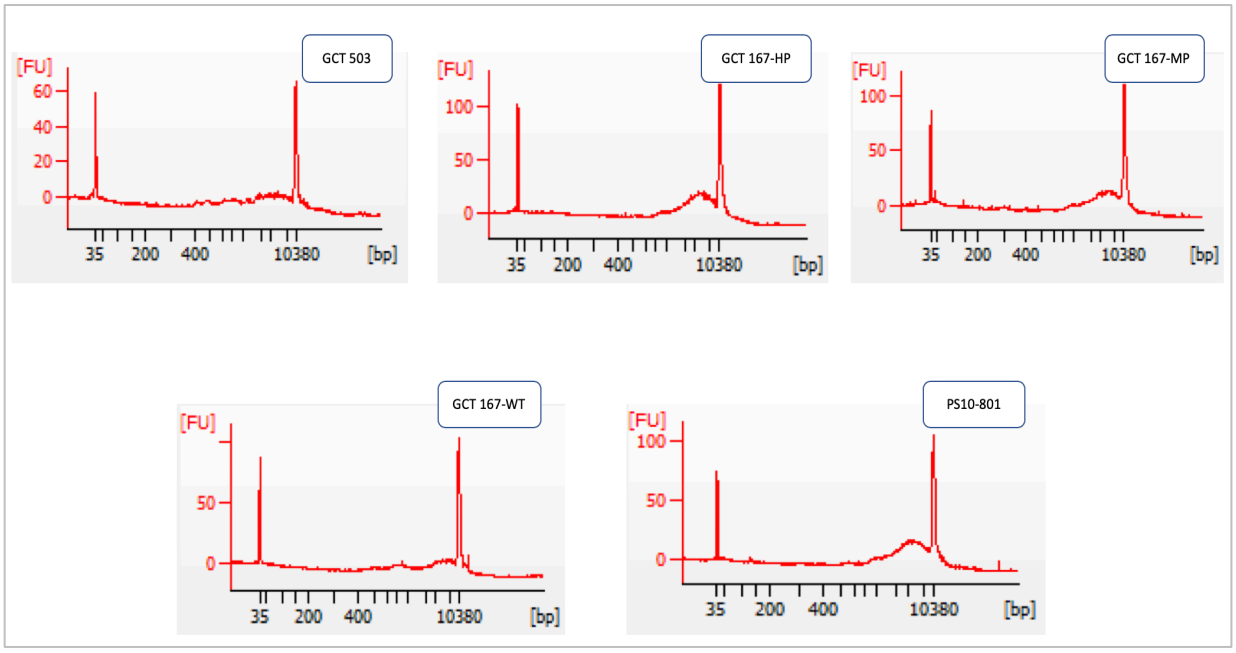

Figure 6.9. Bioanalyzer Data of EV-DNA From all Cell Lines Used in The ddPCR Experiments (N=1).

These findings may represent at least part of the explanation as to why liquid biopsies might be more affective for certain cancers rather than others and point towards including biological and context-specific considerations in developing these assays.

Absence of Oncohistone EV-DNA in Blood of Mice Harbouring H3F3A^{G34W}–Driven Tumours. To establish whether mutant oncohistone DNA can be detected in the plasma of mice bearing GCT lesions with the *H3F3A^{G34W}* mutation, similarly to what we observed for *HRAS* DNA in RAS3 xenografts, a total of six immunodeficient NSG mice were inoculated subcutaneously with immortalized GCT 503 cells suspended in Matrigel. While these cells released low amounts of EV-DNA, they were more tumourigenic than other GCT lines and we reasoned that in addition to active release, other processes such as hypoxia or cell death might contribute to the expected presence of *H3F3A^{G34W}* DNA in blood. Moreover, our earlier studies using RAS3 xenografts revealed sequestration of tumour DNA in white blood cells and an improvement in detection of cancer specific mutations. Thus, once GCT 503 tumours developed, tumour tissue, plasma and buffy coat DNA were extracted. The previously developed ddPCR assay was used in order to detect mutant and wildtype *H3F3A* copies. In tumour tissue, *H3F3A^{G34W}* DNA was readily detected, but no trace of either the mutant or wildtype *H3F3A* alleles were observed in the plasma fraction (Figures 6.10 and 6.11 respectively). Since, as mentioned earlier, our laboratory has recently found that cancer-related mutant ctDNA is often sequestered in circulating white blood cells, especially neutrophils, we also tested the buffy coat layer of these mice for mutant *H3F3A* DNA. However, results obtained were also negative (Figure 6.12) suggesting that, unlike RAS3 tumours, oncohistone-driven GCT xenografts do not efficiently release extracellular DNA into the

circulation.

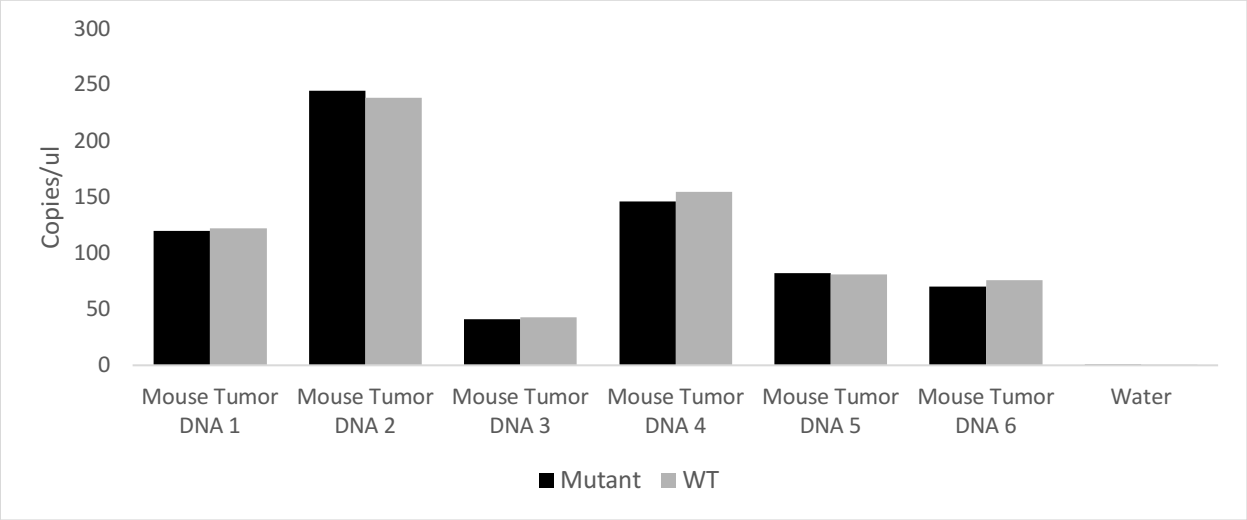

Figure 6.10. ddPCR Test on GCT 503 Tumour-Bearing Mouse Tumour Tissue DNA. Mutant = H3F3A^{G34W} mutant. **WT** = H3F3A^{G34} wildtype.

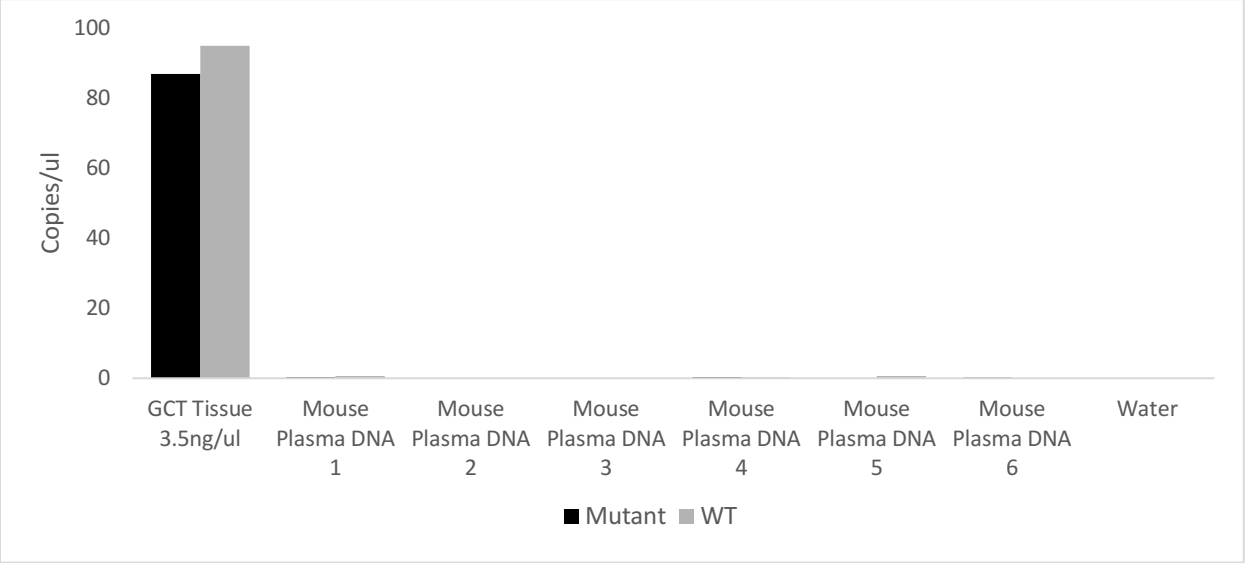

Figure 6.11. ddPCR Test on GCT 503 Tumour-Bearing Mouse Plasma DNA. *GCT Tissue = Patient tumour tissue establishing GCT 503 cell line.* **Mutant** = H3F3A^{G34W} mutant. **WT** = H3F3A^{G34} wildtype.

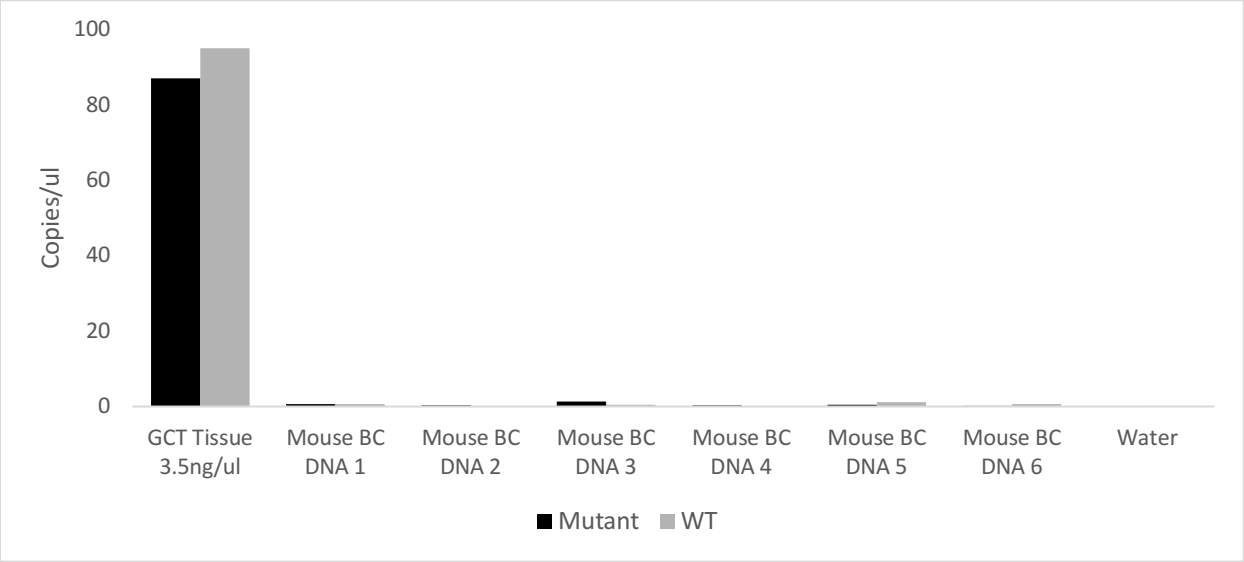

Figure 6.12. ddPCR Test on GCT 503 Tumour-Bearing Mouse Buffy Coat DNA. *GCT Tissue = Patient tumour tissue establishing GCT 503 cell line.* **Mutant** = H3F3A^{G34W} mutant. **WT** = H3F3A^{G34} wildtype.

Furthermore, we had access to one human patient's blood and tumour tissue samples who was diagnosed with giant cell tumor of the bone harboring a *H3F3A*^{G34W} mutation. To this end, we sub-fractionated the blood into its three layers, extracted DNA from the plasma and tumour tissue, and then proceeded using a similar ddPCR assay attempting to interrogate the presence of mutant H3F3A DNA copies in this patient's plasma. The results obtained were negative, as shown in Figure 6.13. Although we did not have access to any more patients, thereby rendering these findings statistically powerless, we believe that GCT lesions may not be efficient in releasing cell-free DNA into the circulation, hence leading us to believe that a ctDNA or EV-DNA liquid biopsy model for this type of cancer is not useful.

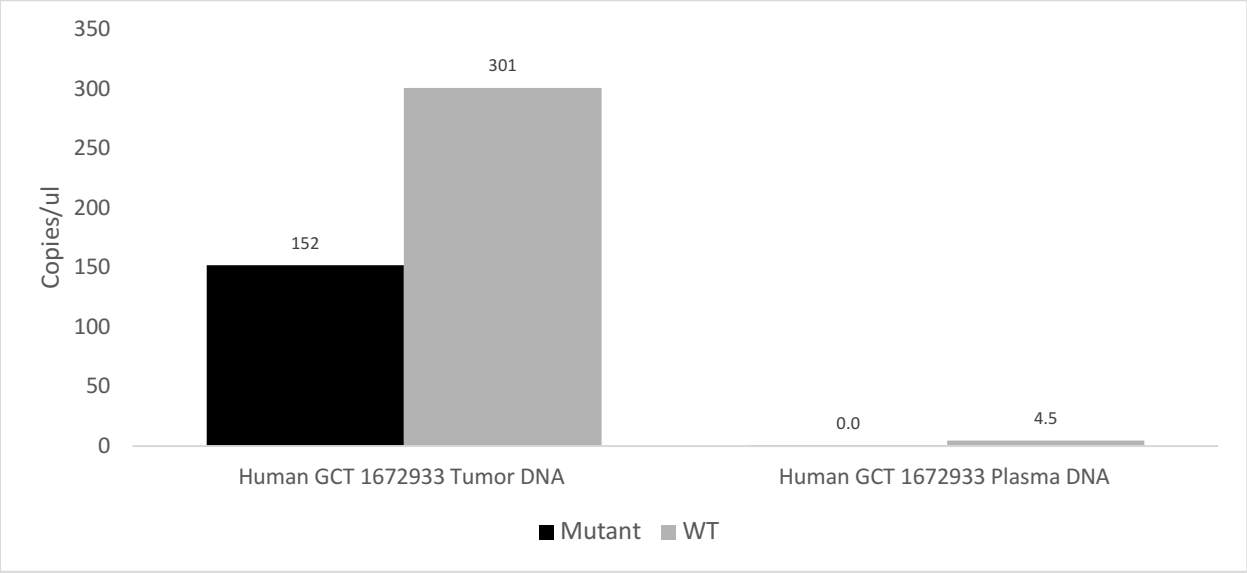

Figure 6.13. ddPCR Test on Human Patient GCT Tissue vs. Plasma DNA. Mutant = H3F3A^{G34W} mutant. **WT** = H3F3A^{G34} wildtype.

Inefficient Release of EV-Associated Oncohistone RNA from GCT Cells In Vitro and In Vivo. While the release of DNA from cancer cells is mechanistically complex and controversial (51), there is a vast body of literature on EV-mediated (or RBP-mediated) release of extracellular RNA, including oncogenic sequences (31, 55). Therefore, we reasoned that the next logical step was to assess oncohistone mutations through a liquid biopsy approach that could be based on mRNA detection. As mentioned previously, EV-RNA was first extracted from conditioned media and cellular RNA was extracted from the cell pellets of all the cell lines in this study to establish the efficiency of this protocol. The isolated RNA was then subjected to a probe-based one-step RT-ddPCR protocol assaying for *H3F3A*^{G34W}. Results shown in Figure 6.14 indicate that the yield of EV-RNA was exceedingly poor. Seemingly, GCT-derived EVs contained less RNA as compared to DNA, a finding that is somewhat contrary to our expectations and requires additional verification.

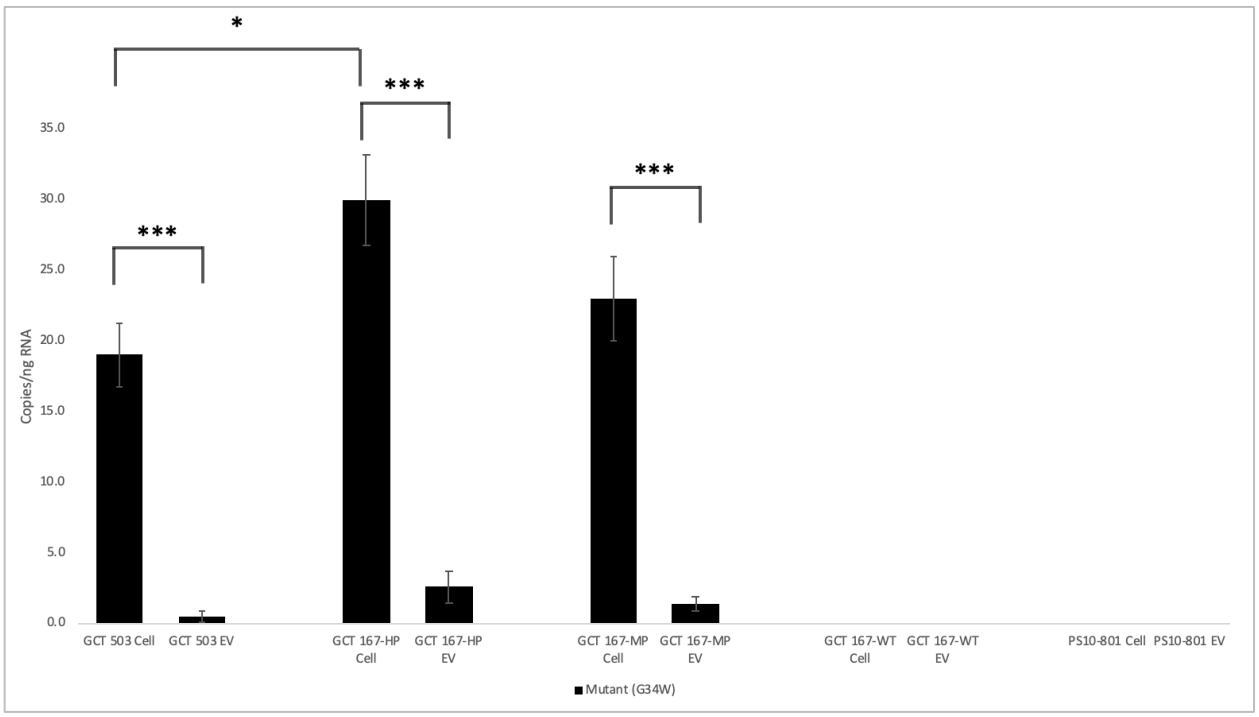

Figure 6.14. One-Step RT-ddPCR Test using mRNA as a Biomarker Platform in Oncohistone-Harboring Cell Lines (N=3). HP = High Passage (> 25), **MP** = Medium Passage (15 < Passage Number < 25), **LP** = Low Passage (< 15). ** = p-value < 0.05, ** =0.05 > p-value > 0.005, *** = p-value < 0.0005.*

In spite of the aforementioned counterintuitive findings, we also examined the content of mutant oncohistone RNA *in vivo*, using blood of mice harbouring GCT-503 xenografts. Similarly, to the DNA detection experiments, RNA was isolated from plasma and buffy coat layers of seven mice and tested for the $H3F3A^{G34W}$ mutation. As observed in the case of DNA, minimal *H3F3A* RNA copies were found in these blood fractions (Figures 6.15 and 6.16). These findings suggest that, unlike in several other tumour models and human cancers, GCT lesions do not efficiently release oncogenic nucleic acid sequences as free molecules or cargo of EVs circulating in blood or even sequestered in neutrophils. We suggest that this pattern is related to the unique biology of these tumours and cells, since in comparable experiments, our group has detected an abundant presence of several mRNAs in the blood of mice bearing glioblastoma lesions (Montermini – unpublished).

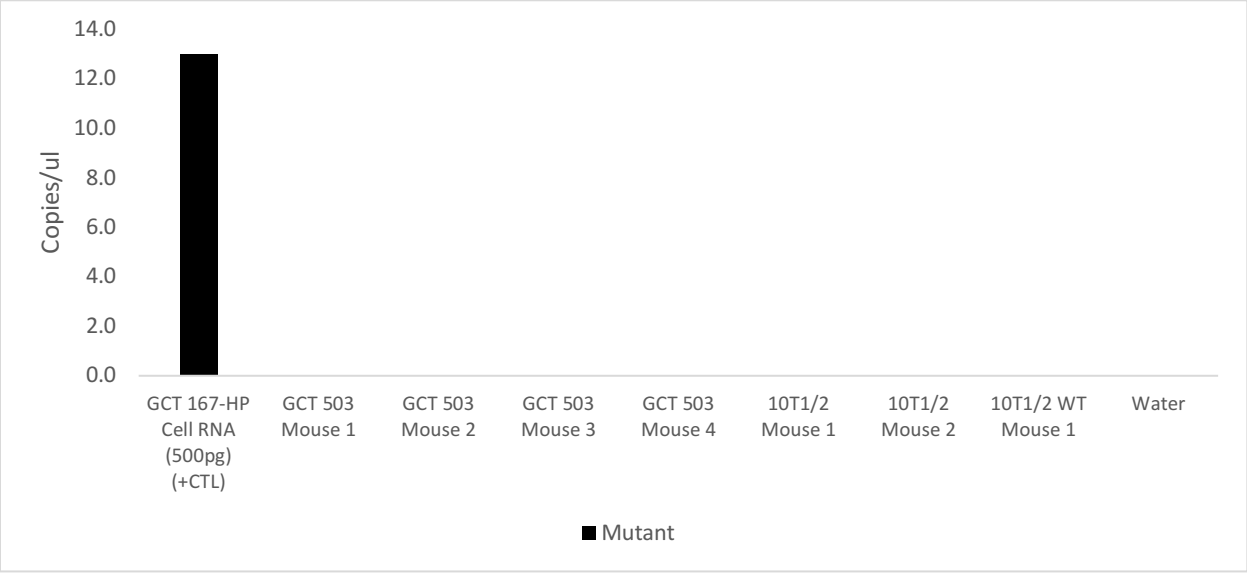

Figure 6.15. One-Step RT-ddPCR Test on GCT-Bearing Mouse Plasma RNA.

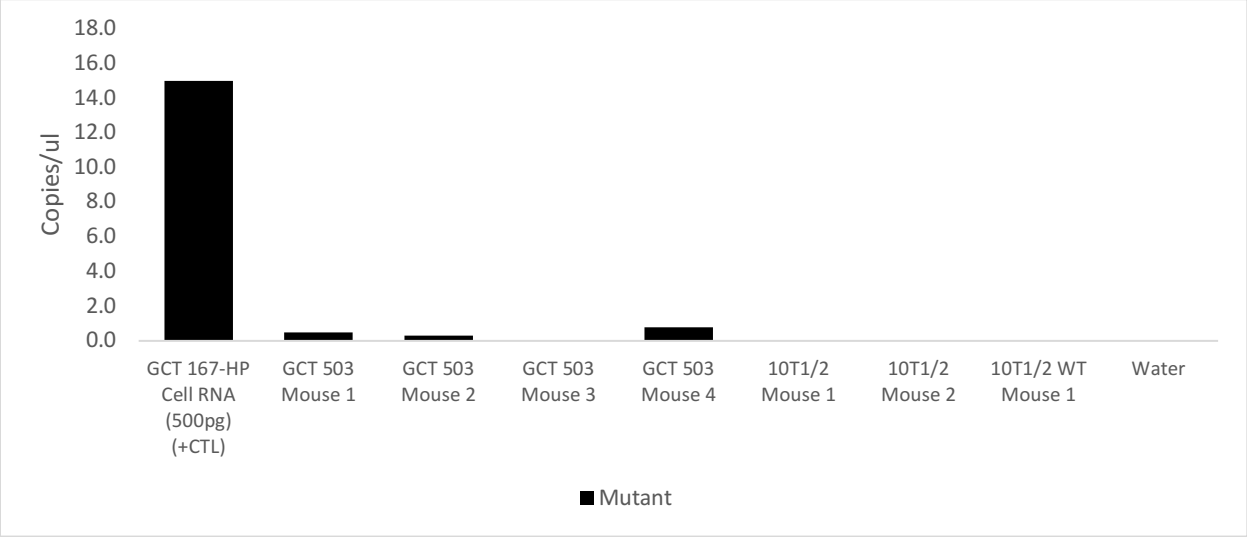

Figure 6.16. One-Step RT-ddPCR Test on GCT-Bearing Mouse Buffy Coat RNA.

Cell-Specific Release Profiles of Oncohistone Proteins From GCT Cell Lines. There is an extensive body of the literature suggesting the cellular release and biological activity of histones (22, 120, 121). It is, therefore, reasonable to suggest that oncohistones may also undergo such a release, either as soluble proteins or as EV-cargo and might be detected in biofluids using mutant-

specific antibodies. These pathways of secretion would likely be different than those constraining our ability to track extracellular histone DNA and RNA. Should this be the case, the biological activity of secretory oncohistones would also present themselves as an interesting and unstudied question.

For these reasons, mutant histone oncoproteins (H3.3$^{G34W/R}$) were the next obvious target of our analysis. In this regard, we performed western blot experiments to assess the presence of mutant H3.3 in EVs. By this line of thought, if mutant H3.3 is detectable in EVs of H3.3 mutant cell lines, then maybe secreted histones, whether they be soluble, nucleosomal or even as cargos of EVs, can be potentially tested in vivo. Figure 6.17 shows the first western blot attempt using cellular histone extracts vis a vis EV-protein lysates from the GCT 503 and GCT 167-HP cell lines, probed for H3.3^{G34W}, total H3 and CD63, a common EV marker.

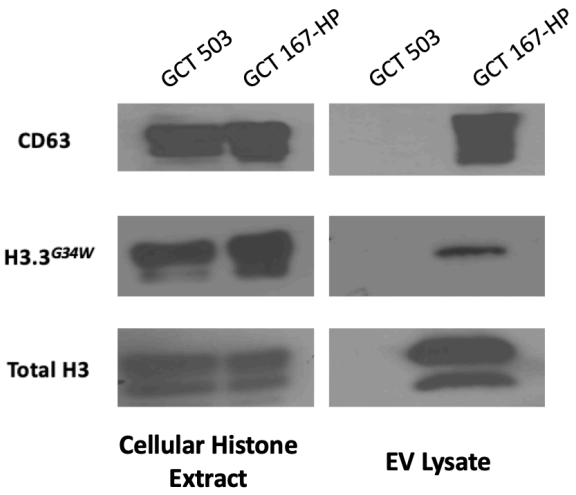

Figure 6.17. Western Blot of Cellular Histone Extracts vs. EV lysates Using Two H3.3^{G34W} Mutant Cell Lines. **HP** = High Passage (> 25). The GCT 167-HP cell line seems to incorporate both mutant and wildtype histone H3 in its EVs qualified by the presence of EV marker CD63. However, the GCT 503 cell line does not seem show similar results even though NTA data (Figure 4.21) indicates that they release small particles.

Interestingly, we observed that at least one cell line (GCT 167-HP) expressed mutant and WT H3.3 in EVs, while the other (GCT 503) did not. To interrogate this unexpected result further, western blot was performed with all the cell lines of interest for this study. Results are reported in Figures

6.18A-C.

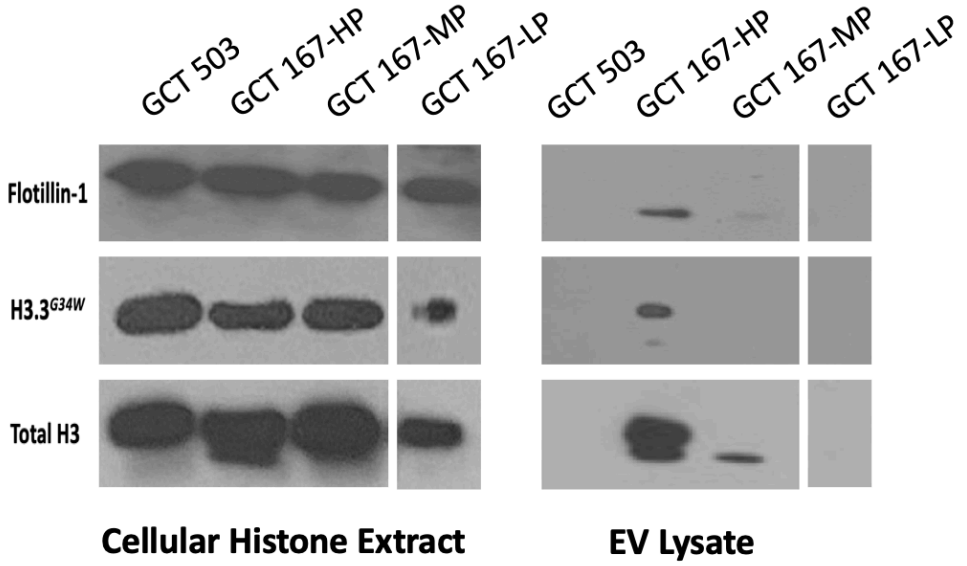

Figure 6.18A. Western Blot of Cellular Histone Extracts vs. EV lysates Using Two H3.3^{G34W} Mutant Cell Lines at Differing Cellular Passage Levels. HP = High Passage (> 25), **MP** = Medium Passage (15 < Passage Number < 25), **LP** = Low Passage (< 15). Once again, the GCT 167-HP cell line shows that mutant H3.3 and total H3 are part of its EV cargo this time qualified by Flotillin-1, a common EV marker. Interestingly, its medium passage counterpart incorporates total H3 and also contains trace amounts of Flotillin-1. No EVs from other cell lines indicate similar observations.

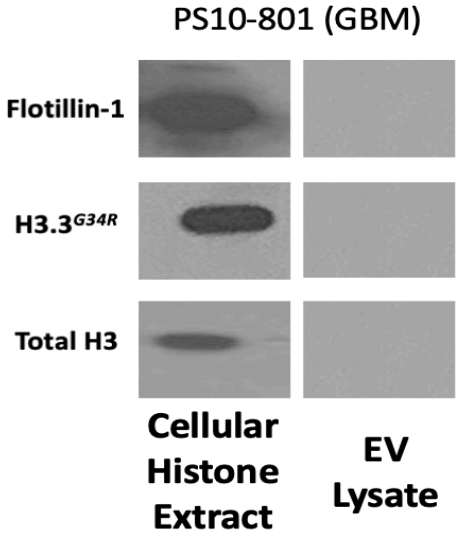

Figure 6.18B. Western Blot of Cellular Histone Extract vs. EV lysate Using a H3.3^{G34R} Mutant Cell Line.

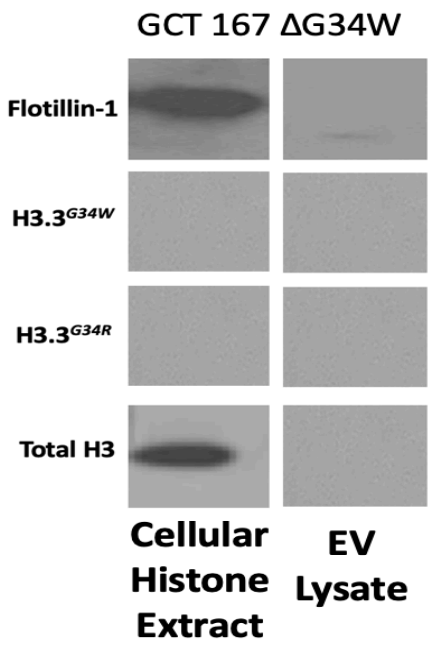

Figure 6.18C. Western Blot of Cellular Histone Extract vs. EV lysate Using a H3.3 Wildtype Cell Line.

Interestingly, once again, the only cell line to have EVs expressing mutant H3.3 is the GCT 167-HP. Also observed, EVs from the GCT 167-HP and GCT 167-MP cell lines seem to carry total H3 (Figures 6.17 and 6.18A). GBM cell line PS10-801, driven by readily detectable H3.3^{G34R} mutation, fails to incorporate this mutant protein into EVs. It should be noted that all these cell lines release ample amounts of particles into conditioned media as detectable by NTA (Figure 6.19), but those particles, quite surprisingly, are devoid of the common EV marker, Flotillin-1 (Figures 6.18A-C).

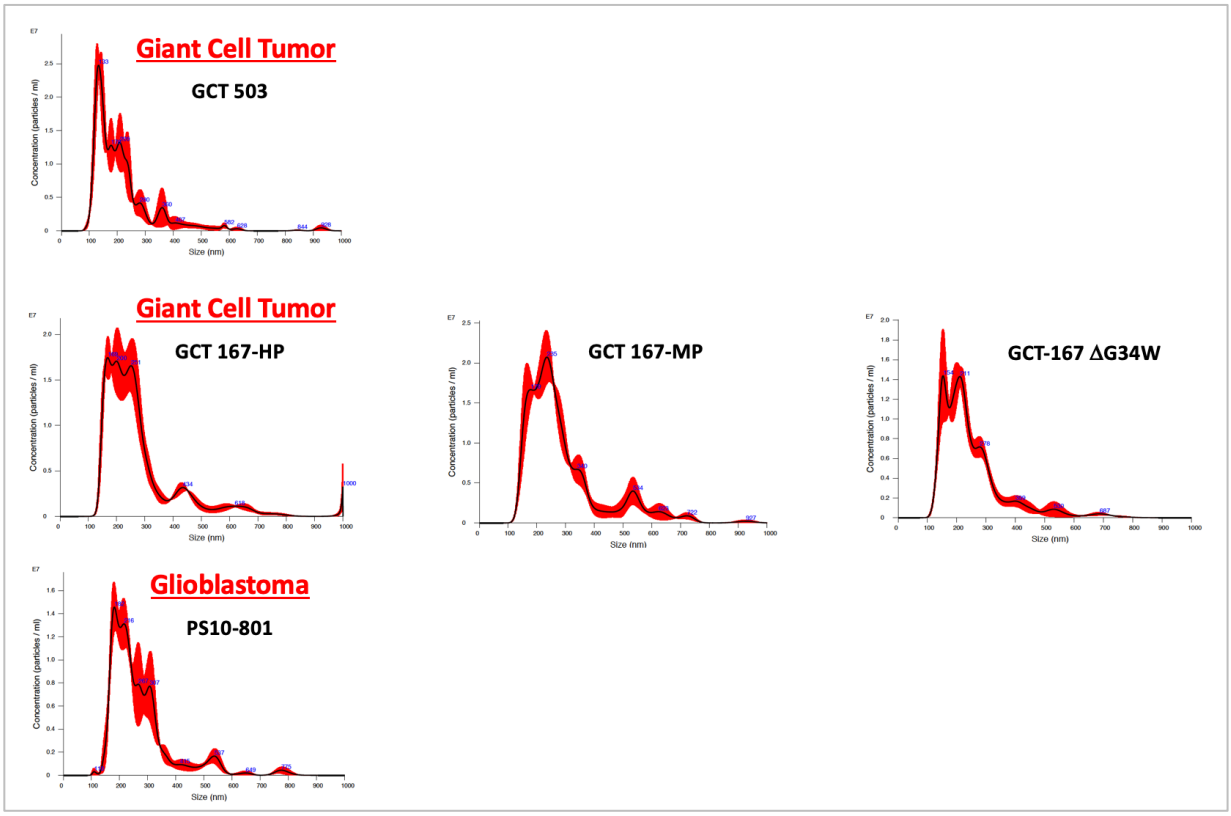

Figure 6.19. NTA data of All Cell Lines Used in Western Blot Experiments (N=1).

Next, as a result of this selective mutant H3.3 protein packaging in EVs between different cell lines, we wanted to interrogate the specific localization of histones, hypothesizing that these DNA-associated proteins are enriched in the EV pellet compared to the soluble flow-through (supernatant). To answer this question, we planned a cell-death ELISA experiment to quantify the presence of nucleosomes in both EV and flow-through fractions. We first employed the GCT 167-HP cell line due to its ability to release EV-H3.3 and we isolated the EV pellet and the supernatant after ultracentrifugation. We then subjected these two fractions to the Cell-Death Detection ELISA^{PLUS} kit (Roche) and generated the results (Figure 6.20).

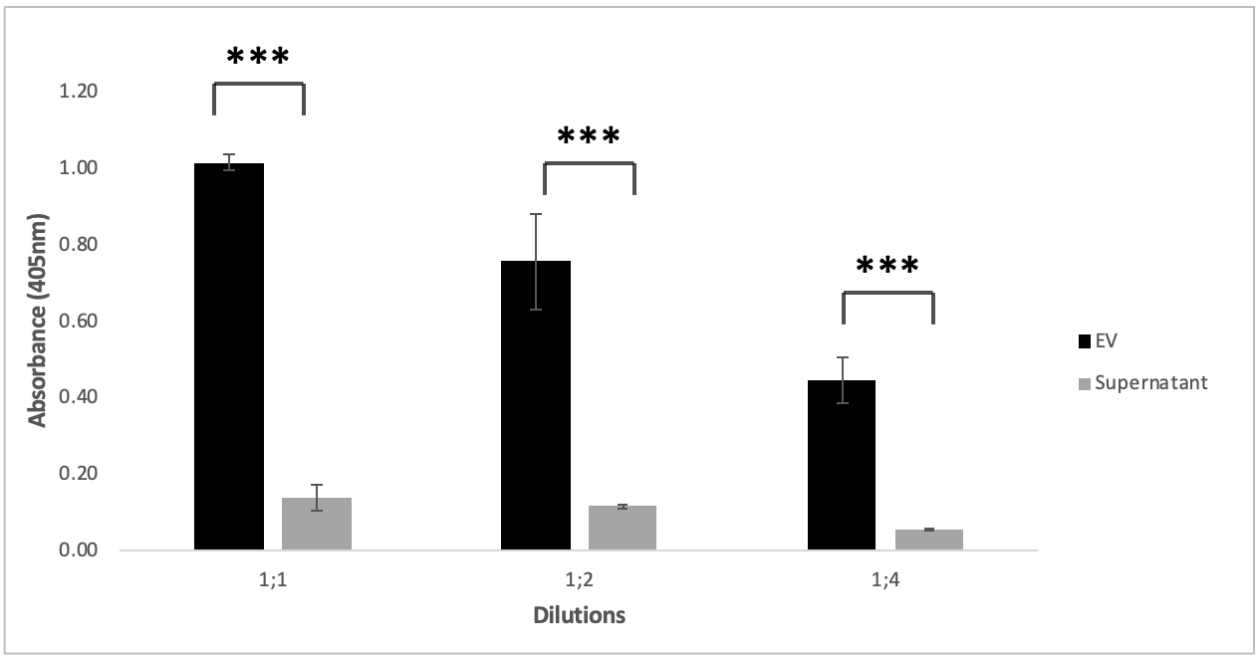

Figure 6.20. Quantification of Nucleosomes in EVs vs. Soluble Fraction by ELISA (N=2). This experiment was done twice (=2). *** = *p-value* < *0.0005*. This ELISA indicates that the highest proportion of nucleosomes are contained in EVs and not in the soluble fraction.

These results clearly document the almost exclusive presence of histones in the EV fraction of tumour cell conditioned media. Only a small proportion of the DNA-histone complex signal was detected in the post-centrifugation supernatant. While this assay is unable to selectively detect mutant H3.3^{G34W}, it is very likely that this oncoprotein is also present in the EV fraction. It would be of considerable interest to explore the biological activity of oncohistone containing EVs.

Collectively, these results indicate that the biology of the different types of cancer cells driven by H3.3$^{G34W/R}$ impedes (or does not facilitate) the EV-mediated secretion of these oncoproteins unless the cells are established in a long-term culture. Even if this is a cell culture artifact, the biology of such release is of interest as it may reveal mechanisms that control EV-mediated chromatin release pathways. Moreover, culture conditions may impose secondary changes in cellular signalling and their vesiculation pathway downstream. Although we were not able to conduct gene expression

analyses comparing the GCT 167-HP, -MP and -LP cell lines, we were able to obtain RNA sequencing data from Dr. Jabado's lab comparing the GCT 503 and GCT 167 cell lines (passage numbers uncertain), as well as data comparing GCT 167 Parental and GCT 167-ΔG34W CRISPR-ed isogenic cell lines (passage numbers uncertain). Tables 6.1A and B summarize these findings by including manually curated genes of interest (histone coding, EV-related and angiogenesis-related genes), the log2 fold change (LFC) of one cell relative to the other and their respective p-values.

Gene	Log2 Fold Change (LFC)	p-value
HIST1H4K	-11.27486534	1.30E-77
HIST1H4J	-10.33754873	9.08E-20
HIST1H2AG	-10.22969822	1.68E-211
HIST1H2BJ	-8.703126796	5.00E-61
HIST1H2AK	-6.887264339	9.67E-107
HIST1H4E	-6.728479291	9.68E-60
HIST1H2BN	-6.03498059	1.87E-26
TSPAN13	-5.575591686	3.44E-28
SERPINE1	-2.824682755	2.46E-08
HIST1H4B	-1.940965034	0.003602677
HIST2H3A	-1.800199442	0.003429595
TSPAN11	-1.406788028	0.002155245
CD9	-1.293113362	0.004552174
ITGA6	1.400593298	2.17E-13
WLS	1.56332635	0.004876967
SYT7	2.153315726	7.84E-05
TGM2	2.485757838	0.000971036
VEGFA	2.558167878	1.42E-06
EPHA1	2.841227089	3.25E-13
CAV1	3.42149168	8.19E-16
ICAM1	4.332464011	8.94E-26
HIST1H1B	7.079723116	3.45E-06

Table 6.1A. Gene Expression Analysis Comparing GCT 503 vs. GCT 167-Parental Cell Lines. A positive LFC indicates gene upregulation in GCT 503 relative to GCT 167 Parental.

Gene	Log2 Fold Change (LFC)	p-value
HIST1H4E	-9.978039099	3.99E-21
HIST1H2AG	-2.870581604	0
SERPINE1	-2.62525237	0
TSPAN13	-2.134847096	4.10E-21
HIST1H2BJ	-1.803417183	7.19E-287
HIST1H2AK	-1.445947751	4.50E-68
HIST1H4B	-1.430937489	1.42E-226
TSPAN11	-1.376977222	4.84E-58
HIST1H4K	-1.259148542	6.47E-131
HIST1H2BN	-1.166992016	6.98E-45
CD9	-1.13894004	1.74E-138
HIST2H3A	-1.109698874	4.35E-05
HIST1H4J	-1.024062836	4.29E-08
EPHA1	1.013892619	1.11E-11
WLS	1.015161325	2.24E-118
ITGA6	1.23248968	1.12E-179
TGM2	1.470243288	1.56E-154
VEGFA	1.571285	0
SYT7	2.061475718	1.44E-19
CAV1	2.340018185	0
HIST1H1B	2.745607282	5.59E-11
ICAM1	3.194374678	0

Table 6.1B. Gene Expression Analysis Comparing GCT 167-WT vs. GCT 167-Parental Cell Lines. A positive LFC indicates gene upregulation in GCT 167-WT relative to GCT 167-Parental.

Interestingly, histone encoding genes seem to be upregulated in the GCT 167 Parental cell line relative to both GCT 503 and GCT 167 WT cell lines. This may partially explain why this cell line packs more histone proteins into its EVs compared to the other two. This table also points out that, since *VEGF*, an angiogenesis-related gene, is downregulated in the GCT 167 Parental cell line compared to its isogenic WT counterpart, tumours derived from this former cell line might not be highly angiogenic, leading us to conclude that nothing more than a sole mutation in one allele of *H3F3A* causes a shift in *VEGF* expression, as is the case for other tumours, even in the absence of

microenvironmental cues (97). Also worthy of mentioning, CD9 and other tetraspanin encoding genes are upregulated in the GCT 167 Parental cell line compared to the GCT 503 cell line. Knowing that these proteins are key markers for EVs, we can start to appreciate that the GCT 167 Parental cell line produces and excretes more EVs relative to its GCT 503 counterpart, which is also evident by looking at the NTA data (Figure 6.19).

In summary, as it was mentioned previously, it seems that the biology of different types of cancer cells driven by oncohistone mutations will affect the EV-mediated secretion of these oncoproteins. To overcome such a limitation, establishing these cells in a long-term culture evidently results in crucial EV-associated gene expression changes, ultimately affecting their vesiculation pathway. While this may be biologically informative and amenable for molecular dissection, the overall conclusion of our studies is that oncohistone-driven tumours do not present themselves as readily accessible for liquid biopsy analyses of their underlying mutations. Therefore, an alternative strategy could be to develop more comprehensive gene expression profiles of these tumours and use EV enrichment to extract diagnostic information.

CHAPTER 7

General Discussion, Conclusions and Future Directions

At the outset, this master's project had the goal of investigating the tumour-related release of oncogenic molecules as an approach to enhance molecular diagnosis of cancers though liquid biopsy. The results obtained have led to several important conclusions.

First, EV-associated DNA may pose a unique challenge to ddPCR detection, unrelated to the total quantity of DNA obtained and likely related to DNA fragmentation or modification. This is true in the case of oncohistone-driven giant cell tumour and glioblastoma cell lines, both in in vitro and in vivo contexts. These findings are in stark contrast to the RAS3 model, in which ample cfDNA is detected in culture material (mainly EVs) in plasma and in the buffy coat layer. These discrepancies are worthy of some consideration as underlying reasons that may or may not be unsurmountable, a determination that directed our interests to other cancer biomarker carriers, such as RNA and proteins.

Second, in our experience, the extraction and analysis of cellular DNA from the mutation-harbouring cell line posed no problem in contrast to EV-DNA. In the latter case, the challenge lies in detection of the sequence-specific signals. Optimization using different primer sets, mutation specific primers or even XNA clamps did not significantly improve the LOD. In the case of EV-DNA extracted from the conditioned media, the LOD is greatly reduced with a large fold-drop in copies/ul, at least for some cell lines. As mentioned earlier, this might be due to the fragmentation of DNA prior to entering EV cargo or presently unknown modifications during EV packaging. It is possible that enrichment of EV content in lipids or carbohydrates may also play some role. Furthermore, mouse plasma and buffy coats were devoid of detectable DNA that carried the

wildtype or mutated *H3F3A* gene. This is partly due to the scarce DNA concentrations in these blood fractions but is also often attributed to cfDNA fragmentation and half-life. Whether these were the reasons for poor detection of oncohistone DNA is presently unknown but intravenous injections of labelled EVs may allow a better assessment of mechanisms that may clear EV-DNA from the circulation (122). Another reason for this observation might be that the experiments in vitro do not always translate to ones in vivo due to unaccounted mechanisms of EV biogenesis, tissue uptake and half-life. In our lab experience, overt release of cfDNA and EV-DNA from cancer cells treated with targeted agents (36, 104) was not matched by a similar signal in blood of tumour-bearing mice harbouring a drug-responsive tumour xenograft of the same cell line {Montermini – unpublished observation}. This difference may suggest that cfDNA in vivo (whether soluble or EV-linked) is often captured by phagocytic cells, as a recent study from our laboratory clearly dictated (38). In addition, the artificiality of the subcutaneous model (with fibrotic and often poorly vascularized structure) is known to inhibit the release of cancer-derived EVs, while similar tumours implanted orthotopically, or at the stage of metastasis, may release ample EVs into the circulation. This is documented by studies on EV-mediated coagulopathy conducted by our lab and others (38, 123). In this setting, different mechanisms of DNA release in vitro versus in vivo, as well as variable EV and cfDNA half-lives might all contribute to the paradoxical results of the xenograft experiments we performed.

Third, we have shown that the type of cell line under study can dictate the amount of EVs released and the associated gDNA (oncogene) content. There is clearly a cell-line/tumour model dependency in detecting cfDNA in vitro and in vivo. This biological variability might be part of clinical inconsistency in the performance of liquid biopsy platforms, which in certain cancers have shown success when it comes to detecting cfDNA, while others may be more problematic (96).

There even exists discrepancies in the experimental setting and the extent of oncogene emission. For example, transformed cell lines may release ample amounts of EGFRvIII, EGFR, RAS or HER2, all of which are membrane associated and strongly transforming (35, 38, 98). On the other hand, leukemic cells driven by the PML-RARA oncogene are extremely inefficient in releasing this oncoprotein and related transcript, even though the EV profiles in these cells exhibit PML-RARA-dependent molecular alterations (124).

In addition, we have noticed that passage number can also be a factor when it comes to DNA, RNA and protein release in the case of oncohistone-driven cell lines. We observed that the GCT 167-HP cell line outperforms in DNA and RNA release using the ddPCR as compared to its medium passage counterpart. While we have no exact or objective measure of the impact of passaging in this case (e.g. telomerase status or alternative telomere lengthening mechanisms, secondary mutations or other events), we have earlier observed the impact of prolonged culturing on EV communication between immortalised astrocytes (98). Furthermore, the GCT 167-HP cell line also exhibits detectable amounts of EV-associated H3.3^{G34W} protein while its earlier passage counterpart does not. While this may reveal some artificial drift in cellular properties, it is also of interest as an isogenic tool to interrogate molecular switches that permit or block export of certain types of EVs (oncogene-containing) versus others. We should also note that oncohistone-driven cancer cells appear to have a peculiar vesiculation profile where high NTA counts are not matched by detection of common markers in EV lysates (e.g. Flotillin-1, CD63). This is unlike other comparable systems studied in our laboratory and elsewhere, including several subtypes of human glioblastoma, epithelial cancers driven by *EGFR* or *RAS*, breast cancer cells and many others. The nature of this property is of great interest.

In regard to future considerations, it would be of our interest to study the biology underlying EV-associated oncohistones. Some questions worthy of answering in the future are:

1) Are there gene expressional differences between the higher and lower passage cell lines that could explain why mutant H3.3 protein is found in EVs of higher passage cell lines? Are these differences biologically and clinically relevant? It would therefore be interesting to perform RNA sequencing experiments on the low to high passage 167 Parental cell lines and interrogate them for gene expressional differences in key histone and EV-related genes.

2) Is there a gene-specific detection differential (cells compared to EVs) for each cell line? In other words, would performing a ddPCR experiment similar to that of Figure 6.8, but in this case using the other genes of interest in this study (*HRAS* and *IDH*), show similar results when comparing cell vs. EV-DNA detection differentials as in the case of the oncohistone mutations?

3) Are oncohistones transmissible horizontally, and to what effect? For example, can a transfer experiment, whereby GCT 167-HP EVs are co-cultured with GCT 167 ΔG34W cells, result in mutant H3.3 expression in the WT cell line? This type of co-culture experiment can also be performed using GCT 167-HP EVs with endothelial cells (HUVEC) and assess for the expression of mutant oncohistones in the former cell line and observe if there are any changes in angiogenesis that would likely be driven by the expression of these mutant oncohistones, for example.

These considerations may aid us in the better understanding of oncohistones in tumorigenesis. The importance of these questions stems not only from the need to develop liquid biopsy assays for inaccessible and highly malignant oncohistone driven-cancers (e.g. DIPG) but also from the virtual absence of knowledge in the intercellular communication pathways and EV trafficking in these tumours. Our project represents the first step in this direction.

References

1. Hanahan D, Weinberg RA. Hallmarks of cancer: the next generation. Cell. 2011;144(5):646-74.
2. Vogelstein B, Kinzler KW. Cancer genes and the pathways they control. Nat Med. 2004;10(8):789-99.
3. Martincorena I, Roshan A, Gerstung M, Ellis P, Van Loo P, McLaren S, et al. Tumor evolution. High burden and pervasive positive selection of somatic mutations in normal human skin. Science. 2015;348(6237):880-6.
4. Downward J. Targeting RAS signalling pathways in cancer therapy. Nat Rev Cancer. 2003;3(1):11-22.
5. Barbacid M. ras oncogenes: their role in neoplasia. Eur J Clin Invest. 1990;20(3):225-35.
6. Wilson JH, Hunt T. Molecular biology of the cell, 4th edition : a problems approach. New York; London: Garland Science; 2002.
7. Serrano M, Lin AW, McCurrach ME, Beach D, Lowe SW. Oncogenic ras provokes premature cell senescence associated with accumulation of p53 and p16INK4a. Cell. 1997;88(5):593-602.
8. Gerlinger M, Rowan AJ, Horswell S, Math M, Larkin J, Endesfelder D, et al. Intratumor heterogeneity and branched evolution revealed by multiregion sequencing. N Engl J Med. 2012;366(10):883-92.
9. Sottoriva A, Barnes CP, Graham TA. Catch my drift? Making sense of genomic intra-tumour heterogeneity. Biochim Biophys Acta Rev Cancer. 2017;1867(2):95-100.
10. Grobner SN, Worst BC, Weischenfeldt J, Buchhalter I, Kleinheinz K, Rudneva VA, et al. The landscape of genomic alterations across childhood cancers. Nature. 2018;555(7696):321-7.
11. Wang X, Prager BC, Wu Q, Kim LJY, Gimple RC, Shi Y, et al. Reciprocal Signaling between Glioblastoma Stem Cells and Differentiated Tumor Cells Promotes Malignant Progression. Cell Stem Cell. 2018;22(4):514-28 e5.
12. Siravegna G, Marsoni S, Siena S, Bardelli A. Integrating liquid biopsies into the management of cancer. Nat Rev Clin Oncol. 2017;14(9):531-48.
13. Dawson MA, Kouzarides T. Cancer epigenetics: from mechanism to therapy. Cell. 2012;150(1):12-27.
14. Flavahan WA, Gaskell E, Bernstein BE. Epigenetic plasticity and the hallmarks of cancer. Science. 2017;357(6348).
15. Morin RD, Mendez-Lago M, Mungall AJ, Goya R, Mungall KL, Corbett RD, et al. Frequent mutation of histone-modifying genes in non-Hodgkin lymphoma. Nature. 2011;476(7360):298-303.
16. Lu C, Ward PS, Kapoor GS, Rohle D, Turcan S, Abdel-Wahab O, et al. IDH mutation impairs histone demethylation and results in a block to cell differentiation. Nature. 2012;483(7390):474-8.
17. Mohammad F, Helin K. Oncohistones: drivers of pediatric cancers. Genes Dev. 2017;31(23-24):2313-24.
18. Schwartzentruber J, Korshunov A, Liu XY, Jones DT, Pfaff E, Jacob K, et al. Driver mutations in histone H3.3 and chromatin remodelling genes in paediatric glioblastoma. Nature. 2012;482(7384):226-31.

19. Behjati S, Tarpey PS, Presneau N, Scheipl S, Pillay N, Van Loo P, et al. Distinct H3F3A and H3F3B driver mutations define chondroblastoma and giant cell tumor of bone. Nat Genet. 2013;45(12):1479-82.
20. Simons M, Raposo G. Exosomes--vesicular carriers for intercellular communication. Curr Opin Cell Biol. 2009;21(4):575-81.
21. Mathivanan S, Ji H, Simpson RJ. Exosomes: extracellular organelles important in intercellular communication. J Proteomics. 2010;73(10):1907-20.
22. Chen R, Kang R, Fan XG, Tang D. Release and activity of histone in diseases. Cell Death Dis. 2014;5:e1370.
23. Crowley E, Di Nicolantonio F, Loupakis F, Bardelli A. Liquid biopsy: monitoring cancer-genetics in the blood. Nat Rev Clin Oncol. 2013;10(8):472-84.
24. Stroun M, Lyautey J, Lederrey C, Olson-Sand A, Anker P. About the possible origin and mechanism of circulating DNA apoptosis and active DNA release. Clin Chim Acta. 2001;313(1-2):139-42.
25. Leon SA, Shapiro B, Sklaroff DM, Yaros MJ. Free DNA in the serum of cancer patients and the effect of therapy. Cancer Res. 1977;37(3):646-50.
26. Stroun M, Anker P, Maurice P, Lyautey J, Lederrey C, Beljanski M. Neoplastic characteristics of the DNA found in the plasma of cancer patients. Oncology. 1989;46(5):318-22.
27. Wang JY, Hsieh JS, Chang MY, Huang TJ, Chen FM, Cheng TL, et al. Molecular detection of APC, K- ras, and p53 mutations in the serum of colorectal cancer patients as circulating biomarkers. World J Surg. 2004;28(7):721-6.
28. Stevens GL, Scheer WD, Levine EA. Detection of tyrosinase mRNA from the blood of melanoma patients. Cancer Epidemiol Biomarkers Prev. 1996;5(4):293-6.
29. Taylor DD, Gercel-Taylor C. MicroRNA signatures of tumor-derived exosomes as diagnostic biomarkers of ovarian cancer. Gynecol Oncol. 2008;110(1):13-21.
30. Chevillet JR, Lee I, Briggs HA, He Y, Wang K. Issues and prospects of microRNA-based biomarkers in blood and other body fluids. Molecules. 2014;19(5):6080-105.
31. Skog J, Wurdinger T, van Rijn S, Meijer DH, Gainche L, Sena-Esteves M, et al. Glioblastoma microvesicles transport RNA and proteins that promote tumour growth and provide diagnostic biomarkers. Nat Cell Biol. 2008;10(12):1470-6.
32. Valadi H, Ekstrom K, Bossios A, Sjostrand M, Lee JJ, Lotvall JO. Exosome-mediated transfer of mRNAs and microRNAs is a novel mechanism of genetic exchange between cells. Nat Cell Biol. 2007;9(6):654-9.
33. Lilja H, Ulmert D, Vickers AJ. Prostate-specific antigen and prostate cancer: prediction, detection and monitoring. Nat Rev Cancer. 2008;8(4):268-78.
34. Felder M, Kapur A, Gonzalez-Bosquet J, Horibata S, Heintz J, Albrecht R, et al. MUC16 (CA125): tumor biomarker to cancer therapy, a work in progress. Mol Cancer. 2014;13:129.
35. Al-Nedawi K, Meehan B, Micallef J, Lhotak V, May L, Guha A, et al. Intercellular transfer of the oncogenic receptor EGFRvIII by microvesicles derived from tumour cells. Nat Cell Biol. 2008;10(5):619-24.
36. Lee TH, Chennakrishnaiah S, Audemard E, Montermini L, Meehan B, Rak J. Oncogenic ras-driven cancer cell vesiculation leads to emission of double-stranded DNA capable of interacting with target cells. Biochem Biophys Res Commun. 2014;451(2):295-301.
37. Peinado H, Aleckovic M, Lavotshkin S, Matei I, Costa-Silva B, Moreno-Bueno G, et al. Melanoma exosomes educate bone marrow progenitor cells toward a pro-metastatic phenotype through MET. Nat Med. 2012;18(6):883-91.

38. Chennakrishnaiah S, Meehan B, D'Asti E, Montermini L, Lee TH, Karatzas N, et al. Leukocytes as a reservoir of circulating oncogenic DNA and regulatory targets of tumor-derived extracellular vesicles. J Thromb Haemost. 2018;16(9):1800-13.
39. Rak J. Extracellular vesicles - biomarkers and effectors of the cellular interactome in cancer. Front Pharmacol. 2013;4:21.
40. Anderson HC. Vesicles associated with calcification in the matrix of epiphyseal cartilage. J Cell Biol. 1969;41(1):59-72.
41. Crawford N. The presence of contractile proteins in platelet microparticles isolated from human and animal platelet-free plasma. Br J Haematol. 1971;21(1):53-69.
42. Trams EG, Lauter CJ, Salem N, Jr., Heine U. Exfoliation of membrane ecto-enzymes in the form of micro-vesicles. Biochim Biophys Acta. 1981;645(1):63-70.
43. Dvorak HF, Quay SC, Orenstein NS, Dvorak AM, Hahn P, Bitzer AM, et al. Tumor shedding and coagulation. Science. 1981;212(4497):923-4.
44. George JN, Thoi LL, McManus LM, Reimann TA. Isolation of human platelet membrane microparticles from plasma and serum. Blood. 1982;60(4):834-40.
45. Kalluri R. The biology and function of exosomes in cancer. J Clin Invest. 2016;126(4):1208-15.
46. Zijlstra A, Di Vizio D. Size matters in nanoscale communication. Nat Cell Biol. 2018;20(3):228-30.
47. Zhang H, Freitas D, Kim HS, Fabijanic K, Li Z, Chen H, et al. Identification of distinct nanoparticles and subsets of extracellular vesicles by asymmetric flow field-flow fractionation. Nat Cell Biol. 2018;20(3):332-43.
48. Abels ER, Breakefield XO. Introduction to Extracellular Vesicles: Biogenesis, RNA Cargo Selection, Content, Release, and Uptake. Cell Mol Neurobiol. 2016;36(3):301-12.
49. Zaborowski MP, Balaj L, Breakefield XO, Lai CP. Extracellular Vesicles: Composition, Biological Relevance, and Methods of Study. Bioscience. 2015;65(8):783-97.
50. Kowal J, Arras G, Colombo M, Jouve M, Morath JP, Primdal-Bengtson B, et al. Proteomic comparison defines novel markers to characterize heterogeneous populations of extracellular vesicle subtypes. Proc Natl Acad Sci U S A. 2016;113(8):E968-77.
51. Jeppesen DK, Fenix AM, Franklin JL, Higginbotham JN, Zhang Q, Zimmerman LJ, et al. Reassessment of Exosome Composition. Cell. 2019;177(2):428-45 e18.
52. D'Souza-Schorey C, Clancy JW. Tumor-derived microvesicles: shedding light on novel microenvironment modulators and prospective cancer biomarkers. Genes Dev. 2012;26(12):1287-99.
53. Choi D, Lee TH, Spinelli C, Chennakrishnaiah S, D'Asti E, Rak J. Extracellular vesicle communication pathways as regulatory targets of oncogenic transformation. Semin Cell Dev Biol. 2017;67:11-22.
54. Lotvall J, Hill AF, Hochberg F, Buzas EI, Di Vizio D, Gardiner C, et al. Minimal experimental requirements for definition of extracellular vesicles and their functions: a position statement from the International Society for Extracellular Vesicles. J Extracell Vesicles. 2014;3:26913.
55. Colombo M, Raposo G, Thery C. Biogenesis, secretion, and intercellular interactions of exosomes and other extracellular vesicles. Annu Rev Cell Dev Biol. 2014;30:255-89.
56. van Niel G, Porto-Carreiro I, Simoes S, Raposo G. Exosomes: a common pathway for a specialized function. J Biochem. 2006;140(1):13-21.

57. Trajkovic K, Hsu C, Chiantia S, Rajendran L, Wenzel D, Wieland F, et al. Ceramide triggers budding of exosome vesicles into multivesicular endosomes. Science. 2008;319(5867):1244-7.
58. Minciacchi VR, Freeman MR, Di Vizio D. Extracellular vesicles in cancer: exosomes, microvesicles and the emerging role of large oncosomes. Semin Cell Dev Biol. 2015;40:41-51.
59. Meehan B, Rak J, Di Vizio D. Oncosomes - large and small: what are they, where they came from? J Extracell Vesicles. 2016;5:33109.
60. Vagner T, Spinelli C, Minciacchi VR, Balaj L, Zandian M, Conley A, et al. Large extracellular vesicles carry most of the tumour DNA circulating in prostate cancer patient plasma. J Extracell Vesicles. 2018;7(1):1505403.
61. Al-Nedawi K, Meehan B, Kerbel RS, Allison AC, Rak J. Endothelial expression of autocrine VEGF upon the uptake of tumor-derived microvesicles containing oncogenic EGFR. Proc Natl Acad Sci U S A. 2009;106(10):3794-9.
62. Di Vizio D, Kim J, Hager MH, Morello M, Yang W, Lafargue CJ, et al. Oncosome formation in prostate cancer: association with a region of frequent chromosomal deletion in metastatic disease. Cancer Res. 2009;69(13):5601-9.
63. Gardiner C, Harrison P, Belting M, Boing A, Campello E, Carter BS, et al. Extracellular vesicles, tissue factor, cancer and thrombosis - discussion themes of the ISEV 2014 Educational Day. J Extracell Vesicles. 2015;4:26901.
64. Cai J, Han Y, Ren H, Chen C, He D, Zhou L, et al. Extracellular vesicle-mediated transfer of donor genomic DNA to recipient cells is a novel mechanism for genetic influence between cells. J Mol Cell Biol. 2013;5(4):227-38.
65. Kahlert C, Melo SA, Protopopov A, Tang J, Seth S, Koch M, et al. Identification of double-stranded genomic DNA spanning all chromosomes with mutated KRAS and p53 DNA in the serum exosomes of patients with pancreatic cancer. J Biol Chem. 2014;289(7):3869-75.
66. Choi D, Montermini L, Kim DK, Meehan B, Roth FP, Rak J. The Impact of Oncogenic EGFRvIII on the Proteome of Extracellular Vesicles Released from Glioblastoma Cells. Mol Cell Proteomics. 2018;17(10):1948-64.
67. Garnier D, Magnus N, Lee TH, Bentley V, Meehan B, Milsom C, et al. Cancer cells induced to express mesenchymal phenotype release exosome-like extracellular vesicles carrying tissue factor. J Biol Chem. 2012;287(52):43565-72.
68. Choi D, Spinelli C, Montermini L, Rak J. Oncogenic Regulation of Extracellular Vesicle Proteome and Heterogeneity. Proteomics. 2019;19(1-2):e1800169.
69. Heijnen HF, Schiel AE, Fijnheer R, Geuze HJ, Sixma JJ. Activated platelets release two types of membrane vesicles: microvesicles by surface shedding and exosomes derived from exocytosis of multivesicular bodies and alpha-granules. Blood. 1999;94(11):3791-9.
70. Morita E, Sandrin V, Chung HY, Morham SG, Gygi SP, Rodesch CK, et al. Human ESCRT and ALIX proteins interact with proteins of the midbody and function in cytokinesis. EMBO J. 2007;26(19):4215-27.
71. Thery C, Boussac M, Veron P, Ricciardi-Castagnoli P, Raposo G, Garin J, et al. Proteomic analysis of dendritic cell-derived exosomes: a secreted subcellular compartment distinct from apoptotic vesicles. J Immunol. 2001;166(12):7309-18.
72. Ratajczak J, Miekus K, Kucia M, Zhang J, Reca R, Dvorak P, et al. Embryonic stem cell-derived microvesicles reprogram hematopoietic progenitors: evidence for horizontal transfer of mRNA and protein delivery. Leukemia. 2006;20(5):847-56.

73. Balaj L, Lessard R, Dai L, Cho YJ, Pomeroy SL, Breakefield XO, et al. Tumour microvesicles contain retrotransposon elements and amplified oncogene sequences. Nat Commun. 2011;2:180.
74. Mittelbrunn M, Gutierrez-Vazquez C, Villarroya-Beltri C, Gonzalez S, Sanchez-Cabo F, Gonzalez MA, et al. Unidirectional transfer of microRNA-loaded exosomes from T cells to antigen-presenting cells. Nat Commun. 2011;2:282.
75. Spinelli C, Adnani L, Choi D, Rak J. Extracellular Vesicles as Conduits of Non-Coding RNA Emission and Intercellular Transfer in Brain Tumors. Non-Coding RNA. 2018;5(1):1.
76. Chevillet JR, Kang Q, Ruf IK, Briggs HA, Vojtech LN, Hughes SM, et al. Quantitative and stoichiometric analysis of the microRNA content of exosomes. Proc Natl Acad Sci U S A. 2014;111(41):14888-93.
77. Akers JC, Ramakrishnan V, Yang I, Hua W, Mao Y, Carter BS, et al. Optimizing preservation of extracellular vesicular miRNAs derived from clinical cerebrospinal fluid. Cancer Biomark. 2016;17(2):125-32.
78. Sansone P, Savini C, Kurelac I, Chang Q, Amato LB, Strillacci A, et al. Packaging and transfer of mitochondrial DNA via exosomes regulate escape from dormancy in hormonal therapy-resistant breast cancer. Proc Natl Acad Sci U S A. 2017;114(43):E9066-E75.
79. Thakur BK, Zhang H, Becker A, Matei I, Huang Y, Costa-Silva B, et al. Double-stranded DNA in exosomes: a novel biomarker in cancer detection. Cell Res. 2014;24(6):766-9.
80. Reifenberger G, Wirsching HG, Knobbe-Thomsen CB, Weller M. Advances in the molecular genetics of gliomas - implications for classification and therapy. Nat Rev Clin Oncol. 2017;14(7):434-52.
81. Webb S. The cancer bloodhounds. Nat Biotechnol. 2016;34(11):1090-4.
82. Haber DA, Velculescu VE. Blood-based analyses of cancer: circulating tumor cells and circulating tumor DNA. Cancer Discov. 2014;4(6):650-61.
83. Krol I, Castro-Giner F, Maurer M, Gkountela S, Szczerba BM, Scherrer R, et al. Detection of circulating tumour cell clusters in human glioblastoma. Br J Cancer. 2018;119(4):487-91.
84. Kros JM, Mustafa DM, Dekker LJ, Sillevis Smitt PA, Luider TM, Zheng PP. Circulating glioma biomarkers. Neuro Oncol. 2015;17(3):343-60.
85. Martinod K, Wagner DD. Thrombosis: tangled up in NETs. Blood. 2014;123(18):2768-76.
86. Wolach O, Sellar RS, Martinod K, Cherpokova D, McConkey M, Chappell RJ, et al. Increased neutrophil extracellular trap formation promotes thrombosis in myeloproliferative neoplasms. Sci Transl Med. 2018;10(436).
87. Mesa MA, Vasquez G. NETosis. Autoimmune Dis. 2013;2013:651497.
88. Abelson S, Collord G, Ng SWK, Weissbrod O, Mendelson Cohen N, Niemeyer E, et al. Prediction of acute myeloid leukaemia risk in healthy individuals. Nature. 2018;559(7714):400-4.
89. Hill AF, Pegtel DM, Lambertz U, Leonardi T, O'Driscoll L, Pluchino S, et al. ISEV position paper: extracellular vesicle RNA analysis and bioinformatics. J Extracell Vesicles. 2013;2.
90. Konoshenko MY, Lekchnov EA, Vlassov AV, Laktionov PP. Isolation of Extracellular Vesicles: General Methodologies and Latest Trends. Biomed Res Int. 2018;2018:8545347.
91. Kwapisz D. The first liquid biopsy test approved. Is it a new era of mutation testing for non-small cell lung cancer? Ann Transl Med. 2017;5(3):46.

92. Shao H, Im H, Castro CM, Breakefield X, Weissleder R, Lee H. New Technologies for Analysis of Extracellular Vesicles. Chem Rev. 2018;118(4):1917-50.
93. Neumann MHD, Bender S, Krahn T, Schlange T. ctDNA and CTCs in Liquid Biopsy - Current Status and Where We Need to Progress. Comput Struct Biotechnol J. 2018;16:190-5.
94. Lim M, Kim CJ, Sunkara V, Kim MH, Cho YK. Liquid Biopsy in Lung Cancer: Clinical Applications of Circulating Biomarkers (CTCs and ctDNA). Micromachines (Basel). 2018;9(3).
95. Cheung AH, Chow C, To KF. Latest development of liquid biopsy. J Thorac Dis. 2018;10(Suppl 14):S1645-S51.
96. Cohen JD, Li L, Wang Y, Thoburn C, Afsari B, Danilova L, et al. Detection and localization of surgically resectable cancers with a multi-analyte blood test. Science. 2018;359(6378):926-30.
97. Rak J, Filmus J, Finkenzeller G, Grugel S, Marme D, Kerbel RS. Oncogenes as inducers of tumor angiogenesis. Cancer Metastasis Rev. 1995;14(4):263-77.
98. Lee TH, Chennakrishnaiah S, Meehan B, Montermini L, Garnier D, D'Asti E, et al. Barriers to horizontal cell transformation by extracellular vesicles containing oncogenic H-ras. Oncotarget. 2016;7(32):51991-2002.
99. Banks WA. The blood-brain barrier as an endocrine tissue. Nat Rev Endocrinol. 2019.
100. Huang TY, Piunti A, Lulla RR, Qi J, Horbinski CM, Tomita T, et al. Detection of Histone H3 mutations in cerebrospinal fluid-derived tumor DNA from children with diffuse midline glioma. Acta Neuropathol Commun. 2017;5(1):28.
101. Stallard S, Savelieff MG, Wierzbicki K, Mullan B, Miklja Z, Bruzek A, et al. CSF H3F3A K27M circulating tumor DNA copy number quantifies tumor growth and in vitro treatment response. Acta Neuropathol Commun. 2018;6(1):80.
102. Viloria-Petit A, Miquerol L, Yu JL, Gertsenstein M, Sheehan C, May L, et al. Contrasting effects of VEGF gene disruption in embryonic stem cell-derived versus oncogene-induced tumors. EMBO J. 2003;22(16):4091-102.
103. Bendre V, Gautam M, Carr R, Smith J, Malloy A. Characterisation of nanoparticle size and concentration for toxicological studies. J Biomed Nanotechnol. 2011;7(1):195-6.
104. Montermini L, Meehan B, Garnier D, Lee WJ, Lee TH, Guha A, et al. Inhibition of oncogenic epidermal growth factor receptor kinase triggers release of exosome-like extracellular vesicles and impacts their phosphoprotein and DNA content. J Biol Chem. 2015;290(40):24534-46.
105. Laird PW, Zijderveld A, Linders K, Rudnicki MA, Jaenisch R, Berns A. Simplified mammalian DNA isolation procedure. Nucleic Acids Res. 1991;19(15):4293.
106. Dou Z, Xu C, Donahue G, Shimi T, Pan JA, Zhu J, et al. Autophagy mediates degradation of nuclear lamina. Nature. 2015;527(7576):105-9.
107. Slater AF. Chloroquine: mechanism of drug action and resistance in Plasmodium falciparum. Pharmacol Ther. 1993;57(2-3):203-35.
108. Liang X, De Vera ME, Buchser WJ, Romo de Vivar Chavez A, Loughran P, Beer Stolz D, et al. Inhibiting systemic autophagy during interleukin 2 immunotherapy promotes long-term tumor regression. Cancer Res. 2012;72(11):2791-801.
109. Morvan J, Kochl R, Watson R, Collinson LM, Jefferies HB, Tooze SA. In vitro reconstitution of fusion between immature autophagosomes and endosomes. Autophagy. 2009;5(5):676-89.
110. Papandreou ME, Tavernarakis N. Autophagy and the endo/exosomal pathways in health and disease. Biotechnol J. 2017;12(1).

111. Hessvik NP, Overbye A, Brech A, Torgersen ML, Jakobsen IS, Sandvig K, et al. PIKfyve inhibition increases exosome release and induces secretory autophagy. Cell Mol Life Sci. 2016;73(24):4717-37.
112. Ojha CR, Lapierre J, Rodriguez M, Dever SM, Zadeh MA, DeMarino C, et al. Interplay between Autophagy, Exosomes and HIV-1 Associated Neurological Disorders: New Insights for Diagnosis and Therapeutic Applications. Viruses. 2017;9(7).
113. Boya P, Reggiori F, Codogno P. Emerging regulation and functions of autophagy. Nat Cell Biol. 2013;15(7):713-20.
114. Chen WW, Balaj L, Liau LM, Samuels ML, Kotsopoulos SK, Maguire CA, et al. BEAMing and Droplet Digital PCR Analysis of Mutant IDH1 mRNA in Glioma Patient Serum and Cerebrospinal Fluid Extracellular Vesicles. Mol Ther Nucleic Acids. 2013;2:e109.
115. S ELA, Mager I, Breakefield XO, Wood MJ. Extracellular vesicles: biology and emerging therapeutic opportunities. Nat Rev Drug Discov. 2013;12(5):347-57.
116. Shankar GM, Balaj L, Stott SL, Nahed B, Carter BS. Liquid biopsy for brain tumors. Expert Rev Mol Diagn. 2017;17(10):943-7.
117. Bettegowda C, Sausen M, Leary RJ, Kinde I, Wang Y, Agrawal N, et al. Detection of circulating tumor DNA in early- and late-stage human malignancies. Sci Transl Med. 2014;6(224):224ra24.
118. Wang Y, Springer S, Zhang M, McMahon KW, Kinde I, Dobbyn L, et al. Detection of tumor-derived DNA in cerebrospinal fluid of patients with primary tumors of the brain and spinal cord. Proc Natl Acad Sci U S A. 2015;112(31):9704-9.
119. Das J, Ivanov I, Montermini L, Rak J, Sargent EH, Kelley SO. An electrochemical clamp assay for direct, rapid analysis of circulating nucleic acids in serum. Nat Chem. 2015;7(7):569-75.
120. Marsman G, Zeerleder S, Luken BM. Extracellular histones, cell-free DNA, or nucleosomes: differences in immunostimulation. Cell Death Dis. 2016;7(12):e2518.
121. Silk E, Zhao H, Weng H, Ma D. The role of extracellular histone in organ injury. Cell Death Dis. 2017;8(5):e2812.
122. Wiklander OP, Nordin JZ, O'Loughlin A, Gustafsson Y, Corso G, Mager I, et al. Extracellular vesicle in vivo biodistribution is determined by cell source, route of administration and targeting. J Extracell Vesicles. 2015;4:26316.
123. Wang JG, Geddings JE, Aleman MM, Cardenas JC, Chantrathammachart P, Williams JC, et al. Tumor-derived tissue factor activates coagulation and enhances thrombosis in a mouse xenograft model of human pancreatic cancer. Blood. 2012;119(23):5543-52.
124. Fang Y, Garnier D, Lee TH, D'Asti E, Montermini L, Meehan B, et al. PML-RARa modulates the vascular signature of extracellular vesicles released by acute promyelocytic leukemia cells. Angiogenesis. 2016;19(1):25-38.